LACP-85-0092
Nuclear Weapon Data
Sigma 1
Critical Nuclear Weapon
Design Information Per
DoD Directive 5210.2
Issued: May 1985

Summary of Classified Research for the Inertial Confinement Fusion Program at Los Alamos National Laboratory (U)

Compiled by
David C. Cartwright
Principal ICF Program Manager

Los Alamos National Laboratory
Los Alamos, New Mexico 87545

SECRET RD

UNCLASSIFIED

INERTIAL CONFINEMENT FUSION OVERVIEW

by David C. Cartwright

INTRODUCTION

The accomplishment of energy gain through nuclear fusion in laboratory experiments will require the solution of a number of interesting, although very complex, scientific and technological problems. Both the Inertial Confinement Fusion (ICF) and Magnetic Fusion Energy (MFE) programs have been somewhat overly optimistic in their initial evaluations of the difficulties involved in controlling nuclear fusion. In both programs, most of the major problems were identified only after the construction and operation of a new (usually more powerful) experimental facility. Researchers in both the ICF and the MFE programs are now trying to build solid technical foundations for their programs so that they can predict results under different experimental conditions. Los Alamos completed construction of the Antares CO_2 laser facility in December 1983 and placed it on operational status for experiments in ICF. Antares, the world's largest operational laser, is the first in a series of new, higher-intensity ICF drivers. The two others in the US are Nova at Lawrence Livermore National Laboratory (LLNL), to be operational in the spring of 1985, and PBFA-II at Sandia National Laboratories (SNL), to begin operation in the fall of 1987. These new facilities will permit experimentation with ICF targets under conditions of temperature and pressure that much more closely similate those required for an energy gain target.

Because Antares has been in operation for more than a year and Helios was operational for 5 years before Antares, it is appropriate to review our present understanding of ICF physics based on CO_2 laser drivers.

[redacted] b(3)

[redacted] b(3)

The ICF mission statement defined for the Los Alamos National Laboratory is as follows:

"The Los Alamos ICF program is one of the main efforts by the Department of Energy (DOE) to evaluate the scientific feasibility of inertially confined fusion, using intense lasers or particle beams to compress and heat small masses of deuterium-tritium fuel to thermonuclear burn conditions. The goals of the national program are:

- *to support nuclear weapons physics research, and*
- *to do research on the potential of inertial fusion for energy production.*

Key technical elements within the ICF program are:

- *the design and confirmation of performance of fuel-filled targets requiring minimum input energy, and*
- *the development of a laboratory driver suitable for driving such targets (at an acceptable cost).*

Whether addressing weapons applications or possible long-term potential as an energy source, there is no significant difference in the short-term program. In the longer term, important scientific and engineering problems would have to be addressed before ICF could be considered for commercial electrical power generation. Since the primary source of the funding is the DOE defense programs, the weapon physics goals will continue to receive emphasis throughout this decade."

SECRET RD

UNCLASSIFIED

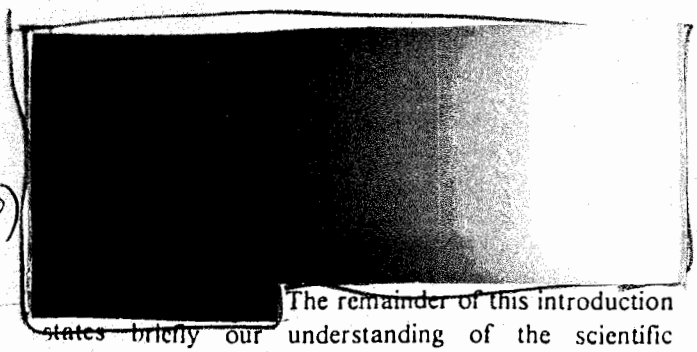

b(3)

The remainder of this introduction states briefly our understanding of the scientific processes governing each step known in the linkage of laser energy to fuel compression in Fig. 1. What is treated as an assertion at this level is explained, and qualified, in the sections that follow.

CHARACTERISTICS OF CO_2 IRRADIATED TARGETS

When high-intensity laser radiation ($>10^{15}$ W/cm^2) strikes a surface, a plasma is formed. For open targets (for example, Fig. 1), the infrared radiation (10.6 μm) produced by the CO_2 laser is absorbed by the plasma through a collective process known as resonant absorption. This process, which we have come to understand primarily through theoretical work, converts all of the absorbed laser energy into energetic electrons. The measured absorption for flat surfaces is about 40%, whereas refraction of the incident light in the plasma reduces measured absorption to about 30% for curved surfaces. To achieve a greater absorption percentage, researchers have designed enclosed targets called "hohlraums" for which the absorption is increased to about 70%.

In open targets, the energetic electrons produced during the resonant absorption process approach temperatures of 80 keV. This distribution of so-called "hot electrons" can exist superimposed on a second "cold" distribution because there are very few collisions in the low-density corona formed around the target. Experiments show that hot-electron temperature increases with laser intensity as $I^{0.4}$. In hohlraum targets, the electron temperatures may exceed 200 keV. The combination of mechanisms responsible for this undesired increase in electron temperature is not yet fully understood, although one of the principal processes appears to be Raman scattering of incident light by oscillations in the low-density plasma filling the interior of the target.

Because all of the energy absorbed from the laser beam initially resides in the hot electrons, it is mandatory to understand the subsequent transport of the electrons to predict how energy can be delivered to other portions of the target. For conditions characteristic of CO_2-laser-driven targets, we have found that very large electric and magnetic fields develop as a result of the large spatial gradients in temperature and density present in the plasma. The magnetic fields are confined to within a few hundred micrometers of the surface and may exceed a megagauss. Consequently, the magnetic forces dominate the motion of most electrons, and their transport is not described by mathematical solutions of the diffusion equations. The self-consistent, theoretical treatment of plasma motion under the influence of an intense laser radiation field has been a major accomplishment by the theorists in this program.

For CO_2 laser intensities exceeding 2×10^{15} W/cm^2, the self-generated magnetic fields become large enough to prevent hot electrons from returning to their origins on the surface defined by the critical plasma density (10^{19} cm^{-3} for 10.6-μm radiation). As a consequence of this magnetically enforced charge separation, ions are accelerated away from the target surface. This ion "blowoff" is not efficient in driving an implosion of the fuel because the momentum per unit energy of the ions is low and represents an energy loss for open targets. The more elaborate geometries discussed in the section on capsule physics attempt to efficiently recover the energy carried by the fast ions.

For good hydrodynamic coupling of momentum to the fuel, the ablation of a large mass at the (low) velocity set by the thermal energy content of the ablator material is required. To achieve energy deposition with a spatial profile shaped to achieve this type of ablation, researchers have turned to the technique used in thermal nuclear weapons; that is, the use of thermal x-ray radiation to drive the implosion. The basic concept in the hohlraum targets is to efficiently convert laser radiation into thermal x-rays. Unfortunately, because of the unexpectedly high electron temperatures discovered in hohlraum targets, the x-ray conversion efficiency is less than 30% when 10.6-μm laser radiation is used as the drive energy source. The reason is that the hot electrons deposit their energy much deeper in the "hohlraum wall" than can be reradiated by a radiation diffusion wave on the time scale of the target implosion. That is, the electrons heat too much mass; hence the temperature of the hohlraum is low, and the resulting conversion to x-ray radiation is inefficient. The efficiency of CO_2-laser-driven hohlraums has been improved by the utilization of the internally generated fields. That is, by reducing the hohlraum wall thickness to a few diffusion depths and

forcing the electrons to recycle through the wall many times (because of the space-charge potentials in the plasma), the energy per unit mass in the hohlraum wall and the radiation temperature are increased substantially. However, the preheat of the fuel by the recycling electrons remains a problem.

To minimize the energy needed to compress the fuel, it is necessary to minimize preheat to an energy level that places the fuel on an adiabat that does not greatly exceed $T \approx 5$ keV at the time of maximum compression. Further refinements are possible only if the central portion of the fuel is elevated to ignition temperatures by properly timed shock collisions. This central portion of the fuel can then serve as a "spark plug" to trigger heating of the remainder of the fuel by local deposition of the α-particles released in the DT reaction.

b(3)

THE CENTURION/HALITE PROGRAM

b(3)

With this record of progress and the number of improvements in technology that have yet to be tried, Centurion/Halite experiments should continue as a mainstay of the ICF program for this decade. Correspondence to the NTS experiments is made by use of the coming generation of laboratory drivers. By measuring the conversion efficiencies described in steps (a) and (b) of Fig. 1, experiments with these machines will define the input required to achieve a certain energy and power of x rays. At the same time, predictive capabilities developed for Centurion experiments along with actual capsule experiments at NTS will reveal what compression and gain can be achieved with the predicted x-ray drive.

b(3)

In the Los Alamos program, we have attempted to capitalize on the great operational advantages of the CO_2 laser, the most efficient and inexpensive high-power laser yet discovered. To develop the next generation driver will require several hundred million dollars of investment. For this reason, all conceivable ways of using the absorbed energy in whatever form that might appear in the target (electrons, ions, x rays, and so forth) are being carefully and systematically explored.

These efforts were reviewed by external panels of experts in 1982 and 1983. In the most recent review, the possible use of the large internal magnetic fields to provide insulation from preheat by hot electrons was suggested. Work in this regard has progressed to the development and computational testing of a novel target that combines advantages of both ICF and MFE by inclusion of magnetic fields for inhibition of electron thermal conduction. This target concept now is being tested using the Antares laser.

As noted above, the achievement of high density is fundamental to all ICF target performance. We have made considerable progress in developing computational techniques that are capable of predicting the extent of instability growth in capsule implosions.

b(3)

The theory requires the experimental determination of coefficients that describe the drag of one fluid mixing into another. Although this is difficult experimentally, Antares may be able to determine information about these coefficients for a variety of material interfaces and thereby improve predictive capabilities for both ICF targets and weapons design.

CONTRIBUTIONS BY ICF TO THE WEAPONS PROGRAM

Almost since its inception, the ICF program has been viewed as a potentially significant contributor to the understanding of the physics of nuclear weapons design. Numerous studies over the years have attempted to

define a role for ICF in weapons physics, identifying the potential for equation-of-state measurements, opacity measurements, thermonuclear burn studies once ignition was achievable, and large-scale x-ray vulnerability facilities once yields approaching 200 MJ were obtained. In recent years, the ICF program has indeed made substantial contributions to the weapons design program. In the last section of this review, an appraisal of the contributions that have been made, and are potentially to be made, is provided. These contributions are summarized below.

b(3)

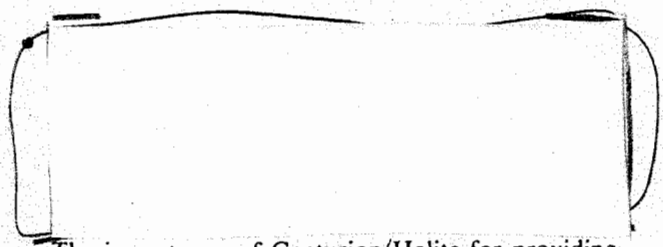

The importance of Centurion/Halite for providing experimental information will continue until laboratory drivers capable of achieving significant thermonuclear burn are developed.

b(3)

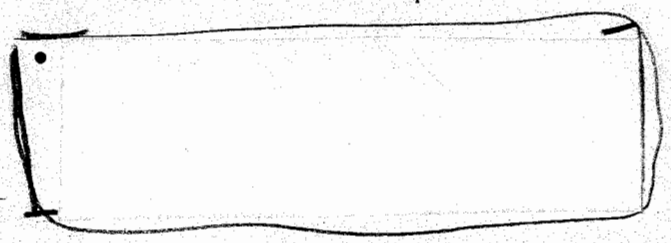

- The national ICF programs would be critical to the US defense program in event of a comprehensive test ban treaty (CTBT) or a limited test ban treaty (LTBT) on nuclear testing.

b(3)

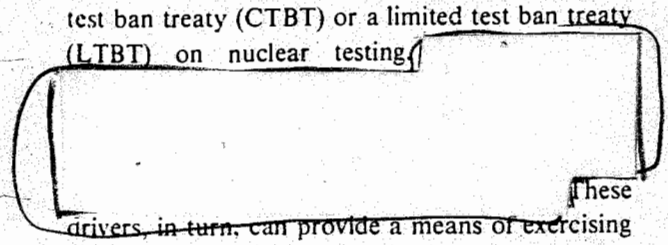

These drivers, in turn, can provide a means of exercising and maintaining design capability under a CTBT as well as a means of addressing the feasibility of fusion itself.

b(3)

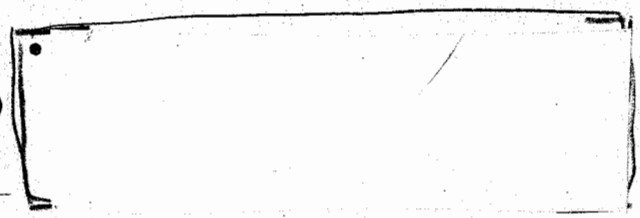

- Improvements in material fabrication developed by ICF have been important ingredients in testing certain x-ray concepts for the Strategic Defense Initiatives (SDI) program.

- The Antares laser facility is a unique source of x-ray and microwave radiation and can be of direct use in studying certain SDI concepts. A future laboratory fusion facility could indeed serve an important function for nuclear vulnerability, lethality, and effects, particularly in the event of a CTBT. The Antares facility has potential for studies on laser radiation cone weapons lethality, and short-pulse, broadband microwave lethality and propagation.

- Measurements of equations of state (EOS) and opacity are now possible in both laboratory laser-driven and underground experiments. Useful confirmation of calculated high-Z opacity in the range of 100-450 eV has been obtained in recent underground tests.

- The physics of rare-gas halide lasers studied in the ICF program is highly beneficial to SDI considerations of laser weapons.

In addition to the early-identified results cited above, both the weapons and ICF programs have benefited from sharing and exchanging personnel. During its 12 years at Los Alamos, the ICF program has attracted many outstanding technical people to the Laboratory, who might not otherwise have come, and helped them develop in technical areas of *direct* interest to the weapons program. Specifically, more than 50 highly skilled staff members have come to work on ICF (or ICF "spin-off" programs) and are now elsewhere in the Laboratory, including at least one Laboratory Fellow and two Associate Directors.

THE FUTURE

Should our attempts to invent a CO_2 laser target that will achieve high-energy gain fail, technology development programs for both a new laser system (KrF) as well as an alternative to all lasers, a heavy ion-beam accelerator, are in progress at Los Alamos. These programs are not so much intended to provide target-shooting capabilities as to establish the cost scaling of these particular systems for potential megajoule-level systems. The research activities in these areas are

UNCLASSIFIED
SECRET/RD

described in the unclassified portion of this two-part review.[1]

Over 10 years of research have taught us a great deal about ICF on a laboratory scale, and it is certainly more difficult than originally envisioned. The inevitable inefficiencies in all the steps between providing incident energy and igniting a fuel have plagued the program.

b(3)

Success would give the ICF program the unique capability of proof of principle before the country is asked to commit to the construction of another driver. In our quest to provide unlimited energy by control of fusion, the workability of ICF should not be overlooked. We are still far from any practical use, but the promise warrants a sustained national effort. For at least the remainder of this decade, we should fully utilize the potential of the research facilities and the technology base we have already established.

REFERENCES

1. D. C. Cartwright, Comp., "Summary of Research for the Inertial Confinement Fusion Program at Los Alamos National Laboratory," Los Alamos National Laboratory report LA-10380 (March 1985).

2. H. G. Ahlstrom, *Physics of Laser Fusion, Vol. II*, "Diagnostics of Experiments on Laser Fusion Targets at LLNL," Lawrence Livermore National Laboratory (January 1982) p. 5.

UNCLASSIFIED
SECRET/RD

UNCLASSIFIED

SECRET/RD

CONTRIBUTIONS BY THE ICF PROGRAM TO THE NUCLEAR WEAPONS PROGRAM AT LOS ALAMOS

by George R. Spillman, William J. Krauser, Thomas A. Sandford, and David C. Cartwright

INTRODUCTION

Almost since its inception, the Inertial Confinement Fusion (ICF) program has been viewed as a potentially significant contributor to the understanding of the physics of nuclear weapons design. Numerous studies over the years have attempted to define a role for ICF in weapons physics, identifying the potential for equation-of-state (EOS) measurements, opacity measurements, thermonuclear burn studies once ignition was achievable, and large-scale x-ray vulnerability facilities once yields approaching 200 MJ were obtained. Recent studies by Los Alamos and Lawrence Livermore National Laboratory (LLNL)[1,2] have reviewed the potential for significant contributions to the weapons program by the ICF laser facilities, and a recent study[3] summarized specific experiments that could be conducted at the Antares facility in support of Strategic Defense Initiatives (SDI). In recent years, the ICF program has made substantial contributions to the weapons design program. In this report a realistic appraisal of the contributions that have been made, and that are potentially to be made, is provided. These contributions are summarized below.

b(3)

- The importance of Centurion for providing experimental information will continue until laboratory drivers capable of achieving significant thermonuclear burn are developed.

b(3)

- The national ICF programs would be critical to the US defense program in the event of a comprehensive test ban treaty (CTBT) or a limited test ban treaty (LTBT) on nuclear testing.

b(3)

These drivers, in turn, can provide a means of exercising and maintaining design capability under a CTBT as well as a means of addressing the feasibility of fusion itself.

b(3)

- Improvements in material fabrication developed by ICF have been important ingredients in testing certain x-ray concepts for the SDI program.

- The Antares laser facility is a unique source of x-ray and microwave radiation and can be of direct use in studying certain SDI concepts. A future laboratory fusion facility could indeed serve an important function for nuclear vulnerability, lethality, and effects, particularly in the event of a CTBT. The Antares facility has potential for studies on laser radiation cone weapons lethality and on short-pulse, broadband microwave lethality and propagation.

- Measurements of EOS and opacity are possible underground and have been done. Useful confirmations of calculated high-Z opacity in the range 100-450 eV have been obtained.

SECRET/RD UNCLASSIFIED

b(3)

b(3)

It is significant that postshot results are in nearly perfect agreement with the preshot predictions.

It is expected that increasing use of these techniques will be made in future design efforts.

b(3)

laser vulnerability data in the high-fluence range of importance have been obtained with Gemini (built as a CO_2 ICF laser), Aurora (Los Alamos KrF laser), and Sprite (UK KrF laser).

Antares produces copious bremsstrahlung gamma rays and microwaves as a unique source for vulnerability and lethality studies. Gamma-ray output of 600 J in a bremsstrahlung spectrum characterized by a 0.6-MeV temperature in a 1-ns pulse has been observed at Antares (>0.5 TW gamma-ray power). This could be a unique capability for exploring radiation cone vulnerability and lethality.

b(3)

The microwave power output is expected to be much greater than 1 GW based upon Helios observations, and attempts to characterize the output are continuing.

Materials and Fabrication

Many materials and fabrication technologies developed for the ICF program have found important uses in various parts of the Los Alamos weapons program. A summary is presented below.

- *Foams.*

b(3)

- *Thin Metallic Foils.*

b(3)

b(3)

- *Precision Machining.* Another use for thin foils has been in the area of NTS diagnostics. Our Fast Transit Plasma Measurement Group used the development of multilayer stacks for x-ray measurement detectors and is considering this development of precision machining and characterization has largely been motivated and funded by ~~tization has largely been motivated and funded by~~ ICF. This capability is now used by a variety of laboratory programs.

b(3)

- *Laser Welding.*

b(3)

Additionally, ICF funds developed the technology now being used by the new cw-CO_2 laser welder to develop processes for welding plutonium and other actinides.

- *Coatings.* The technology for applying precise layers of radiochemical layers upon various weapon device shells was an adaptation of coating technology developed for ICF projects. This application has been used many times in weapon tests such as Dolcetto and Coalora.

- *Beryllium Technology.* ICF has funded the development of hot isostatic pressing (HIP) of beryllium at Battelle Laboratory, and we will have this technology transferred here by spring of 1985.

b(3)

Diagnostics

This resolution represents a factor of 4 improvement over the resolution of the conventional PINEX used for weapons physics diagnostics. Central to this improvement is a new uniform taper design, 50-μm-diam pinhole, which requires an innovative combination of metalworking technologies (precision vapor deposition, electroforming, electric discharge machining, and conventional precision machining) to fabricate.

- *Precision Alignment of PINEX Rack Geometry.*

Distortion of the rack following alignment and downhole placement can adversely affect the actual geometry at shot time.

This alignment performance will no doubt be useful for planning diagnostics for future weapons tests.

- *Tri-head Detectors.*

Some of these improvements have been incorporated in PINEX systems for weapons diagnostics. Neutron data from these detectors can be used to derive the average temperature of the thermonuclear burn and are also sensitive to the models used to calculate burn performance (and instabilities).

- *PINEX Imaging Fluor Improvements.* Rarex, an imaging fluor, has been used in some PINEX applications to weapons tests because of its high light emission.

Although a small innovation, this will almost certainly be useful for certain weapons PINEX applications.

- *Advanced Diagnostics.* Although we rely primarily on the advanced technologies being developed for weapons diagnostics to improve Centurion ICF diagnostics, it is anticipated that some advances made to meet special ICF requirements will be available for the weapons program sooner than if there were no Centurion program.

-

CTBT/LTBT Considerations

In the event of an LTBT or a (zero-fission) CTBT, a major concern for the national defense would be how to maintain some weapons design expertise and to be able to determine if significant advances in weapons are being made by other parties during the ban.

Under a comprehensive test ban, maintenance of expertise in secondary design would be particularly difficult. An ICF (or other pure fusion) program provides

SECRET/RD

almost the only substantial method of exercising secondary design talent and comparing calculations with experimental results.

(b)(3) [redacted] Even a minimal level of testing would help preserve design expertise. Some experimental input may be crucial to retaining a core staff able to resume conventional design and testing, if deemed necessary. Another crucial contribution of ICF in a CTBT could be the vulnerability/lethality testing capability that could be provided by a laboratory fusion facility as discussed earlier.

REFERENCES

1. G. Spillman, J. Brownell, G. Fraley, and D. Giovanielli, "Report of the Weapons Physics Experiments Group," Los Alamos National Laboratory memorandum P-DO/82-GRS-3 (March 1982).

2. C. T. Alonso et al., "Proposals for Laboratory Weapons Physics Experiments," Vol. 1, Executive Summary, Lawrence Livermore National Laboratory report UCRL-53293, Vol. 1, M-3679 (May 30, 1983).

3. D. C. Cartwright, D. Forslund, D. Gill, G. McCall, and F. Morse, "Applications of the Antares Laser Facility," Los Alamos National Laboratory memorandum DRP/FRA:DCC:004 (January 1985).

570-3-420

SECRET/RD

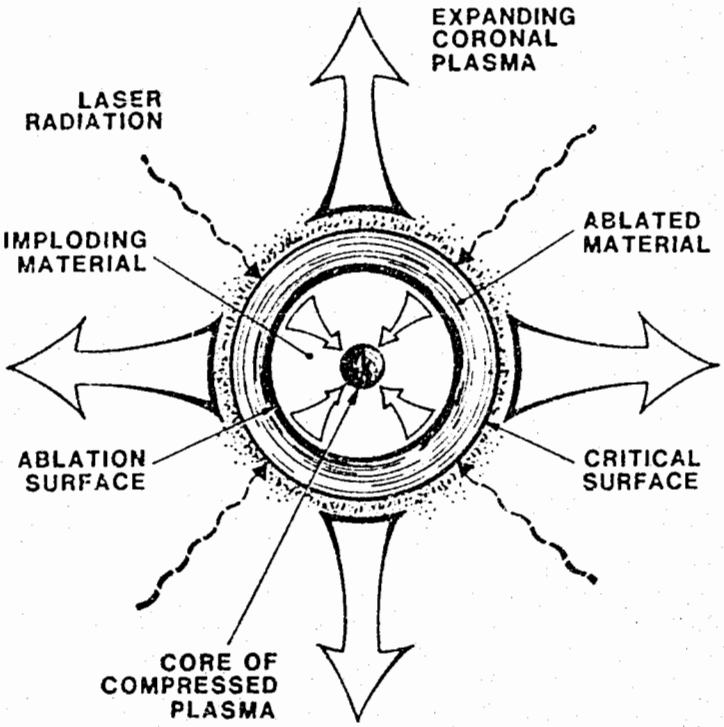

Fig. 1. Schematic for basic concept of DT capsule implosion.

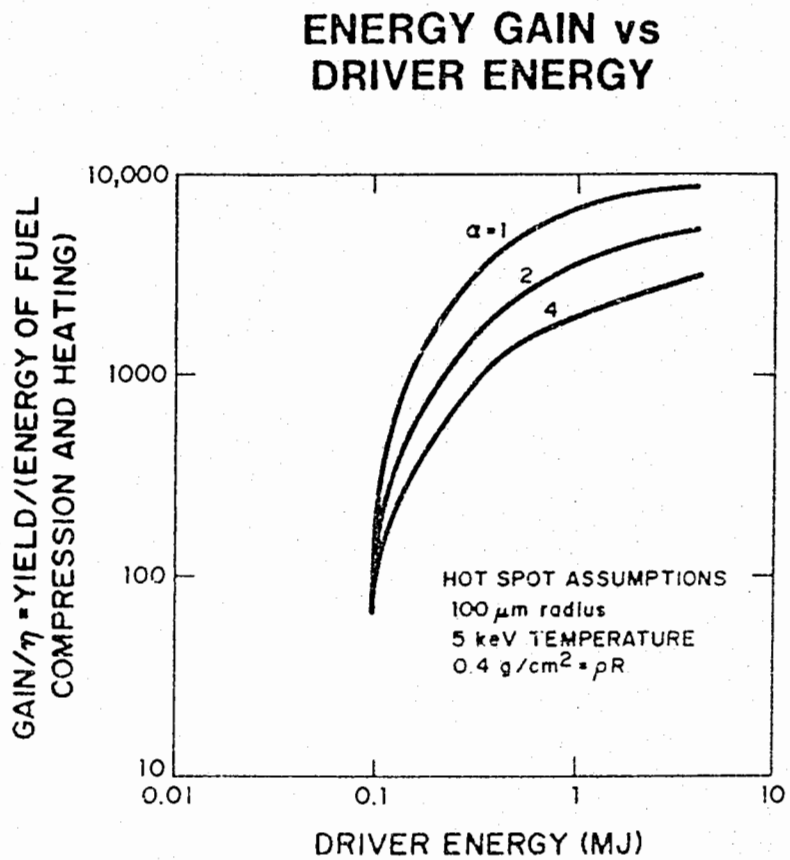

Fig. 2. Energy of fuel compression and heating.

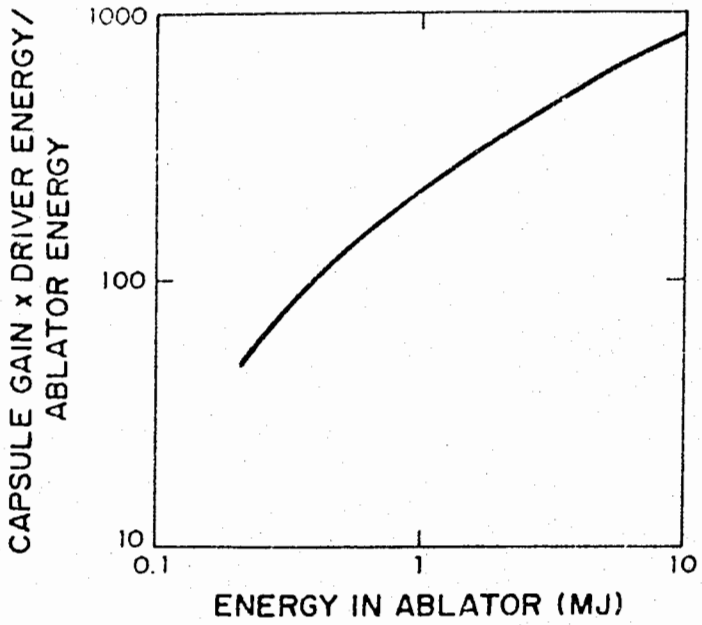

Fig. 3. Best estimate of capsule gain as a function of driver energy.

of pusher material into fuel, and limitations on minimum shell thicknesses. Hydrodynamics of unstable fluids is the least predictable aspect of the implosion and ignition physics and is expected to continue to be a major research concern of ICF for the foreseeable future.

Small Amplitude Theory

In this section, we begin by discussing the instability at a planar interface between two incompressible fluids of infinite extent and then discuss the effects of spherical geometry, finite extent, and compressibility.

The basic concept of hydrodynamic instability is illustrated by the instability inherent in a dense fluid in a gravitational field supported by a light fluid, or equivalently, a dense fluid accelerated by a light fluid.[4] If a dense, incompressible fluid of infinite extent is bounded along a surface that is planar except for a sinusoidal perturbation of wavelength λ and amplitude $a \ll \lambda$, the amplitude will change (as long as it remains small) under the gravitational acceleration (g) according to the equation

$$\frac{d^2a}{dt^2} = \sigma^2 a \quad ,$$

where σ is defined from

$$\sigma^2 \cong \frac{2\pi\, g\alpha}{\lambda} \quad ,$$

and α is the Atwood number defined by the densities (ρ^1, ρ^2) on either side of the interface,

$$\alpha \cong \frac{\rho_1 - \rho_2}{\rho_1 + \rho_2} \quad ,$$

and the product $g\alpha$ is taken as positive when the acceleration is in the direction from light fluid to dense fluid. Two cases of particular interest are those of a sudden, impulsive acceleration $[g = \pm v\delta(t)]$ and a constant acceleration. If we start from an initial amplitude, a_0, rate of change, $\dot{a}_0$, integration of the growth equation gives

$$\dot{a}(t) = a_0 2\pi a v/\lambda + \dot{a}_0 \text{ , and}$$
$$a(t) = (a_0 2\pi a v/\lambda + \dot{a}_0)t + a_0$$

for impulsive acceleration, or

$$a(t) = a_0 \cosh \sigma t + \frac{\dot{a}_0}{\sigma} \sinh \sigma t \quad (\sigma^2 > 0)$$

$$= a_0 \cos |\sigma| t + \frac{\dot{a}_0}{|\sigma|} \sin |\sigma| t \quad (\sigma^2 < 0)$$

for constant acceleration.

From these equations, note the following.

- The effect of an impulsive acceleration on an initially stationary perturbation is growth (Richtmeyer-Meshkov instability). If the acceleration is from light to dense fluid, an amplitude reversal occurs.

- A constant acceleration from heavy to light is stabilizing. In the case of an implusive acceleration followed by a constant acceleration from heavy to light fluid, the linear growth is limited to an envelope

$$|a| < a_0 \left(1 + \sqrt{\frac{2\pi a}{\lambda g}}\, v \right) .$$

  where, as before, v is the impulsively delivered interface velocity.

- An acceleration from light to heavy fluid leads to exponential growth (Rayleigh-Taylor instability). This growth generally is much faster than that due to impulsive acceleration in a capsule, but at the pusher/fuel interface the time available for the impulsively driven growth may be much longer than that for decelerative growth.

The instability problem as we have discussed it so far has been limited to the perturbed planar interface between two infinite incompressible fluids. ICF capsules are not planar, incompressible, or infinite.

Finite shell thickness may allow interface perturbations to propagate all the way through a shell; that is, the shell may break up. Also, the perturbation in fluid motion is not limited to the interface.

For an incompressible planar fluid layer of thickness d, which has an initial perturbation on side 1 that grows because of an acceleration to amplitude a_1 and a side 2 that is initially smooth, an amplitude a_2 will develop on side 2 given by[3]

$$\frac{a_2(t)}{a_1(t)} \simeq e^{-2\pi d/\lambda} .$$

Therefore, a perturbation may grow at an interface that would be described as stable from infinite medium calculations; that is, the perturbation can feed through from one interface to another.

Perturbations at a converging interface in the absence of accelerations will grow (to maintain the volume of the perturbation for incompressible flow).[4] For impulsively accelerated interfaces, the result of convergence of a spherical interface from radius R_0 to $R = R_0/C_R$ is a multiplication of the growth by a factor

$$C_R(C_R + 1)/2 .$$

Compressibility is sometimes estimated in terms of uniform compression in which the perturbations are simply compressed, or decompressed, with the material. The finite sound speed in compressible fluids also results in transient oscillations for a few sound transit times over a wavelength. This may be of particular importance for feedthrough of perturbations in thin shells.

Large-Amplitude Instability Growth and Mix

As the perturbation wavelength becomes large (comparable to a wavelength), the growth becomes more complex and difficult to predict from *ab initio* theory. The growth slows, the shape becomes distorted by shear instabilities (Kelvin-Helmholz) because of relative motion of the two fluids, and perturbations of different wavelengths interact with one another. First, we discuss the asymptotic behavior of single-wavelength perturbations and then discuss the effects of the presence of more noisy initial perturbations that give rise to multiple modes (wavelengths) and mode interaction.

As the perturbation grows in the Rayleigh-Taylor instability, it develops into a buoyantly rising bubble of light material penetrating dense material and spikes of dense material penetrating light. The bubbles rise with a velocity that is constant for constant acceleration given by

$$v_B \sim \sqrt{g\lambda} ,$$

where the proportionality constant is a weakly varying function of the density ratio across the interface. For an infinite density ratio, the spike penetrates to the free-fall

line, the position the interface would have reached if the acceleration had been zero. For finite density ratio, shear instability along the spike deforms the spike, blunting it into a "mushroom" shape, which, from 2D hydrodynamics simulations, in the far asymptotic region penetrates at a rate proportional to but larger than the bubble velocity. The ratio of bubble to spike growth is also a function of density.[5]

The theory of asymptotic multimode growth is based upon dimensional and heuristic arguments, 2D hydrodynamics simulations, and a few experiments.

Dimensional and heuristic arguments suggest that, at an interface, two fluids subjected to a constant acceleration will mix turbulently so that the dominant perturbation wavelength (λ_D) in the mix region and the thickness of the mixed region (ℓ_m) both grow in time:

$$\lambda_D \sim f(\rho_1/\rho_2)gt^2 \text{ and}$$
$$\ell_m \sim h(\rho_1/\rho_2)gt^2 .$$

Note the consistency with the bubble growth formula for single modes for which

$$v_B \sim \sqrt{g\lambda} .$$

The mechanism for λ_D to increase with time is thought to be vortex combination. The increase of λ_D with time is expected from 2D turbulence theory, but is not so clearly expected from 3D turbulence theory.

For slowly varying acceleration, one might argue from the linear equations that to preserve the correct growth parameter the factor gt^2 should be replaced by

$$\left[\int \sqrt{g}\, dt\right]^2 .$$

For impulsive acceleration, we note that the preceding equation for ℓ_m is derivable from

$$\frac{d^2\ell_m}{dt^2} \sim gh(\rho_1/\rho_2) ,$$

and for $g = v\delta(t)$ we could integrate to obtain

$$\ell_m \sim h(\rho^1/\rho^2)gt .$$

Not only are the forms of these equations *ad hoc*, but coefficients are required to use them in a quantitative way. The 2D hydrodynamics simulations and a few experiments with incompressible fluids indicate that a reasonable choice is

$$\ell_m = a_B + a_s ,$$
$$a_B \simeq 0.07\ \alpha gt^2 , \text{ and}$$
$$a_s \simeq (1.5 \text{ to } 2.5)x\ a_B ,$$

where a_B is the distance of penetration of light fluid into heavy and a_s is the distance of penetration of heavy fluid into light.

Bubble penetration, as calculated from the above formula, typically exceeds that calculated for a single mode by the time the single-mode growth is a wavelength.

The form of equations to be integrated within hydrodynamic codes is different from that above and will be discussed very briefly in a subsequent section.

THE RESEARCH PROGRAM IN IMPLOSION PHYSICS

Summary and Introductory Comments

In the preceding sections, we presented a discussion of simplified phenomenology of implosion physics. In this section, we concentrate on discussion of research that addresses the phenomenology in quantitative detail.

We generally believe that we can calculate idealized hydrodynamics well (no instabilities), including radiation flow and electronic heat conduction.

b(3)

We still have to demonstrate the capabilities for fuel ignition and substantial gain at low driving temperatures and energy, but it is probable that such demonstration and the achievement of high gain will be more dependent upon further development of our understanding of unstable hydrodynamics and mix rather than on substantial changes in our understanding of idealized (stable) hydrodynamics.

We have made substantial progress in the understanding of unstable hydrodynamics and mix in the past few years.

b(3)

b(3)

An unstable hydrodynamics experimental program is planned at the Antares laser to provide the necessary input and represents a new approach to mixing, which promises the potential of a breakthrough in predictive capability.

b(3)

The achievement of this goal requires improvements in ideal hydrodynamics efficiency by pulse shaping and more and more quantitative, detailed understanding of unstable hydrodynamics as we proceed to the lower driving temperatures and energies corresponding to ICF. Fortunately, the two aspects of the problem, improved ideal hydrodynamic efficiency and control of instabilities, appear to be compatible. As we noted in the previous section, continued acceleration at the pusher-fuel interface as required for efficient compression is also stabilizing.

b(3)

However, as we have also discussed, problems may arise due to instabilities at other interfaces. Ultimate capsule design may involve very careful tradeoffs among various aspects of the instability problem, idealized efficiency, and aspects of the capsule drive.

The theoretical gain curve of Fig. 3 includes *judgment* of the constraints imposed by instability growth and mix. As judgment is replaced by understanding, the replacement for this curve may be more optimistic or more pessimistic.

The Calculation Techniques

Idealized (Stable) Hydrodynamics—The LASNEX Code. LASNEX is the workhorse code of ICF.

b(3)

b(

The more sophisticated, and less well understood, physics aspects associated with coupling to the driver are more *ad hoc* and parameterized.

Much fusion design work incorporated instability considerations through lore, such as

- mix follows the "free-fall line" (extends into fuel from zero-order interface to $\int\int g dt' dt$)
- do not allow free-fall line to penetrate more than ϵ of fuel,
- require that fuel calculate to ignite with inner ϵ dudded,
- turn off yield calculation when the second reflected shock reaches the pusher,
- perturbations grow only during the "unstable" phase (when acceleration is from light to dense material),

- perturbations of wavelength λ grow up from initial perturbations of wavelength λ,
- the most dangerous wavelength is one comparable to a shell thickness,
- the shell aspect ratio ($r/\Delta r$) should be limited to some maximum, and
- the convergence ratio (r_0/r) should be limited to some maximum.

[redacted]

b(3)

[redacted]

Global Perturbation Theory (Small Amplitude Growth)—The DOC and SACI Codes. A more nearly complete way to treat instability growth in the small amplitude regime is via first-order perturbation theory. In the DOC code,[7] the radiation diffusion or conduction and hydrodynamics equations are solved as a zero-order solution (idealized, stable hydrodynamics) obtained from a standard radiation hydrodynamics code plus a first-order spherical harmonic perturbation. The solution of perturbation variables is on the whole mesh rather than just at interfaces, which gives the propagation and transient behavior of disturbances throughout the mesh due to perturbations introduced anywhere in the problem. As noted above, the perturbation technique allows consistent solution of the hydrodynamics equations with equations of energy transfer as well.

The basic limitation of perturbation theory codes is limitation to small amplitude. Even with a first-order perturbation, there is currently some controversy over possible neglect of terms, and there is some suggestion that existing perturbation codes may not be reproducing the Richtmeyer-Meshkov instability.

The SACI code is being written to provide a new and careful look at first-order perturbation theory. It is demonstrating reproduction of the Richtmeyer-damped oscillation about the incompressible-like interface solution for shocks. Additionally, it is showing transient behavior (oscillations) propagating away from the interface, which may present worse interface coupling problems than predicted from incompressible theory.

SACI is also predicting greater pusher/fuel interface instability growth with increasing implosion velocity.

[redacted]

b(3)

A drop in performance at lower velocities is believed to be due to preburn temperature, which is too low. It is tantalizing to associate the performance drop at higher velocities with the SACI-predicted instability growth, but this cannot yet be confidently done.

At present, SACI does not include the equations of radiation diffusion, and this will be part of the continued development.

[redacted]

b(3)

As a result, experiments are required to provide coefficients for the phenomenological equations and also to check upon assumptions of functional dependence.

Post-processing codes have been developed by Youngs and Roberts,[8] AWRE, and Burke and Rupert, LLNL.

[redacted]

b(3)

SECRET/RD

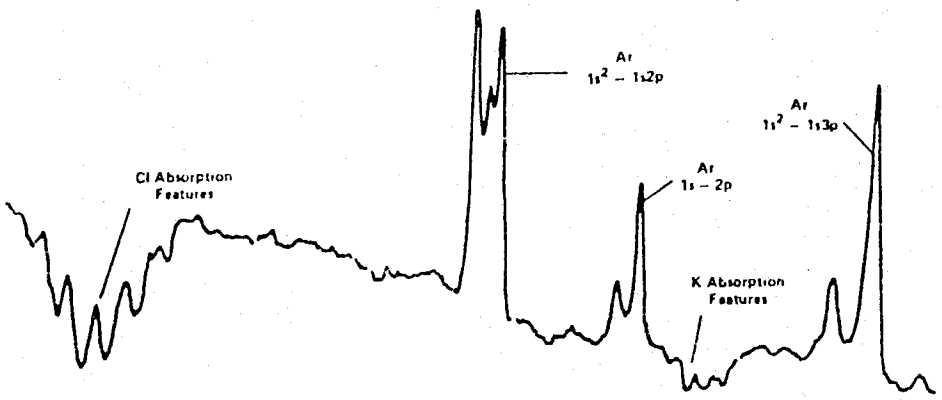

Fig. 5. A typical observed spectrum that shows K, Cl in absorption only.

670 0033

SECRET/RD

b(3)

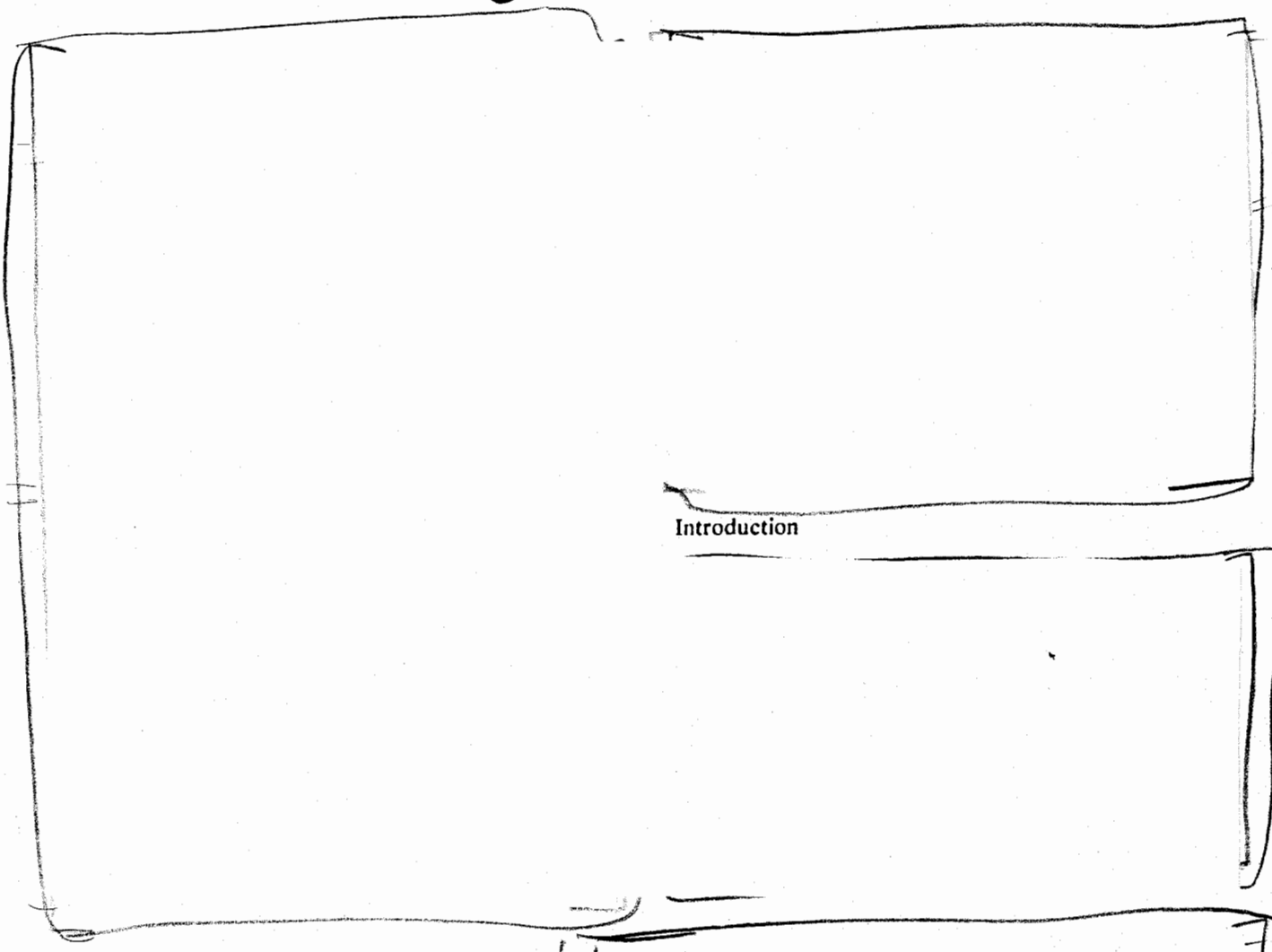

Introduction

b(3)

b(3)

b(3)

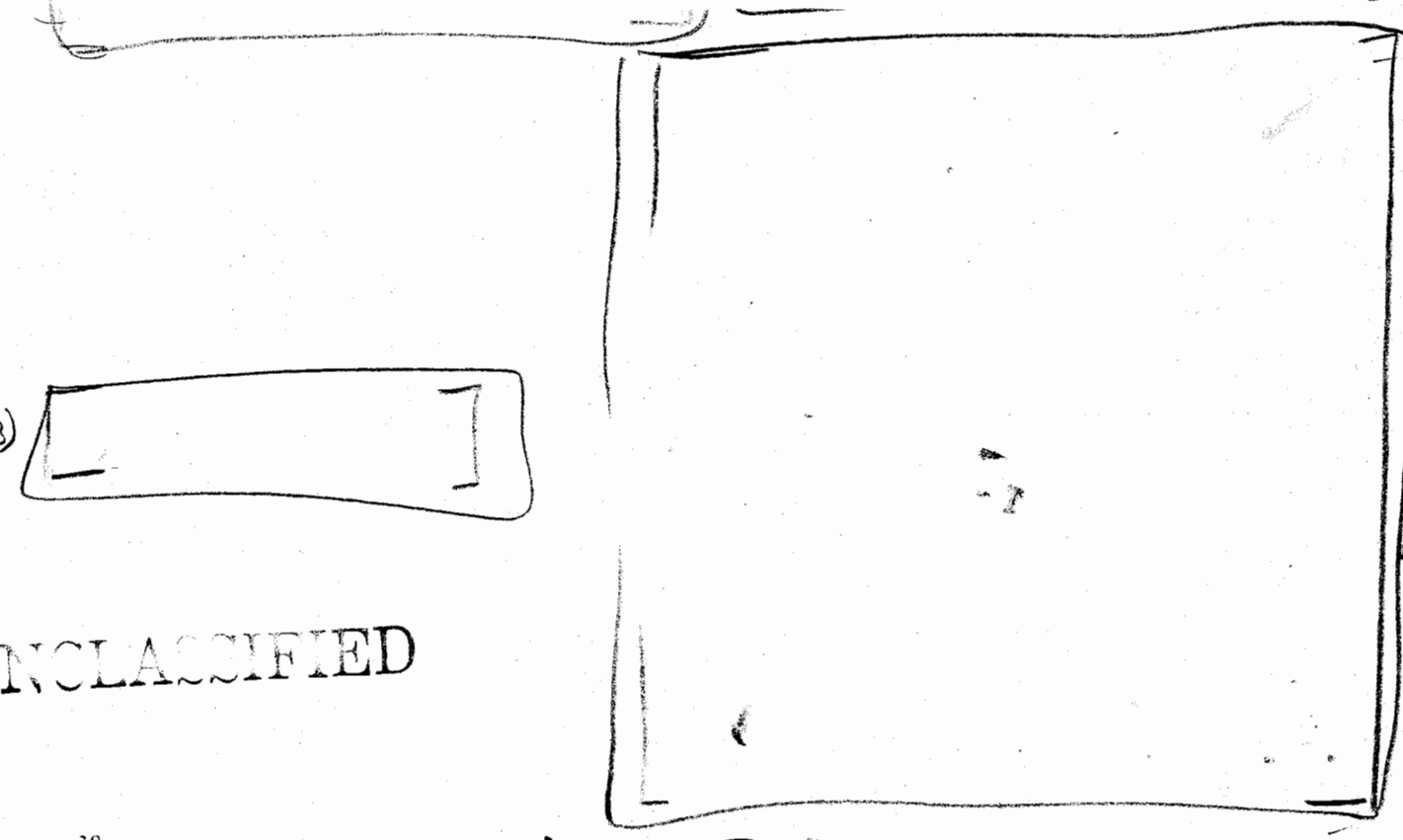

6 7 0 4 0 3 3 6

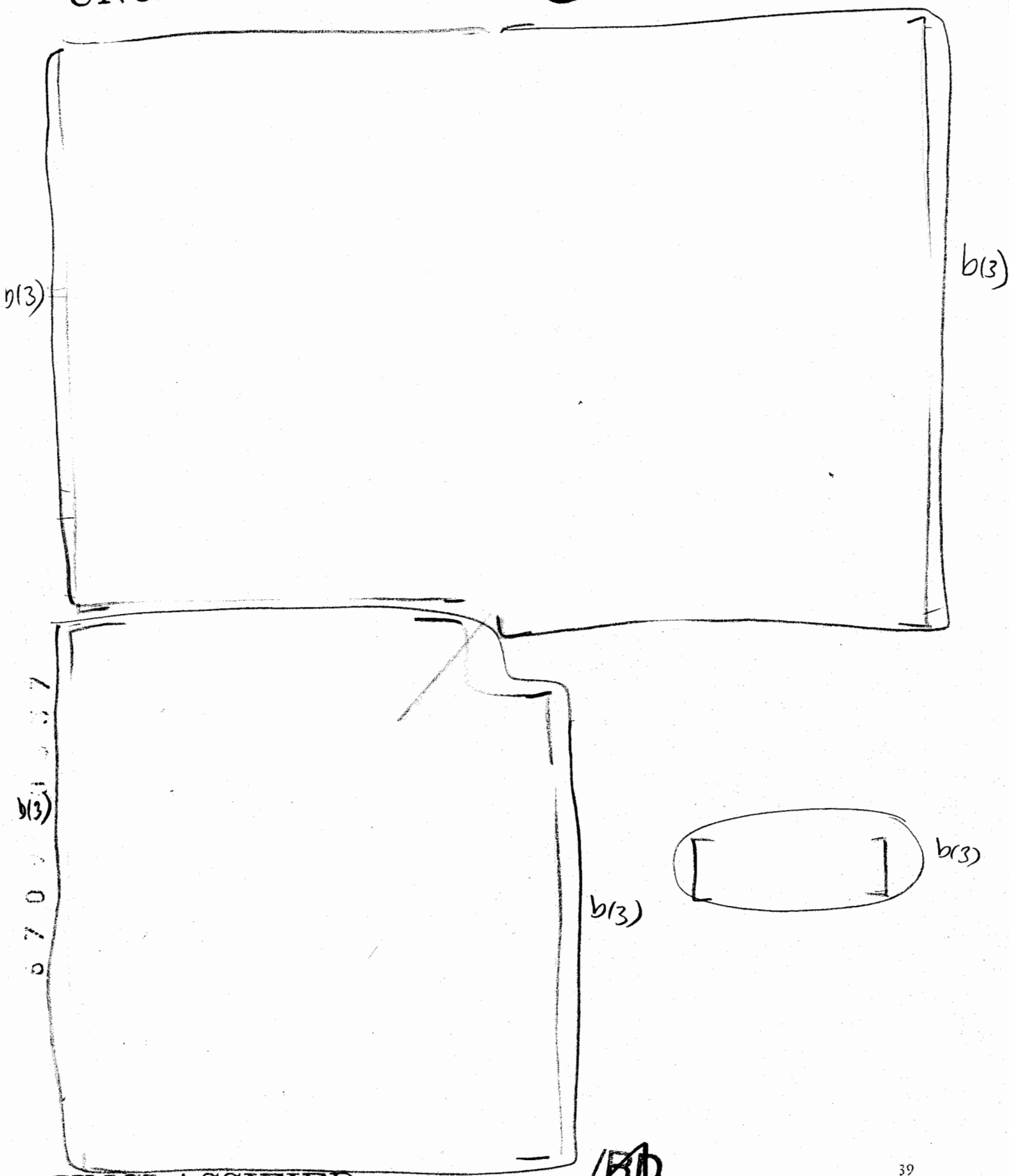
b(3)
b(3)
b(3)
b(3)
b(3)

b(3)

b(3)

Each laboratory will participate in the other's event.

b(3)

These are but two examples of the fine collaboration that exists between the Centurion and Halite programs.

b(3)

Before being shipped to the NTS, the rack was placed in a tower at Zia where LOS pipe installation and initial alignment took place. Next, cabling, terminal boards, local shielding, junction boxes, and some detectors were installed. Performing these tasks at the Los Alamos rack fabrication and alignment facility reduced rack time in the tower at NTS and was a worthwhile economic measure.

Designing a Standard Underground Test

b(3)

The elaborate character of these tests required extensive engineering to field each test.

b(3)

Although Los Alamos and Livermore could each design an NTS experiment to satisfy these objectives, we felt that there were tremendous advantages to using the same design at both Laboratories. Each Laboratory has different technologies and different approaches to NTS diagnostics and rack and tower design.

b(3)

With these factors established as being common to both Laboratories, each designed the rest of the experiment in its most cost-effective manner.

b(3)

b(3)

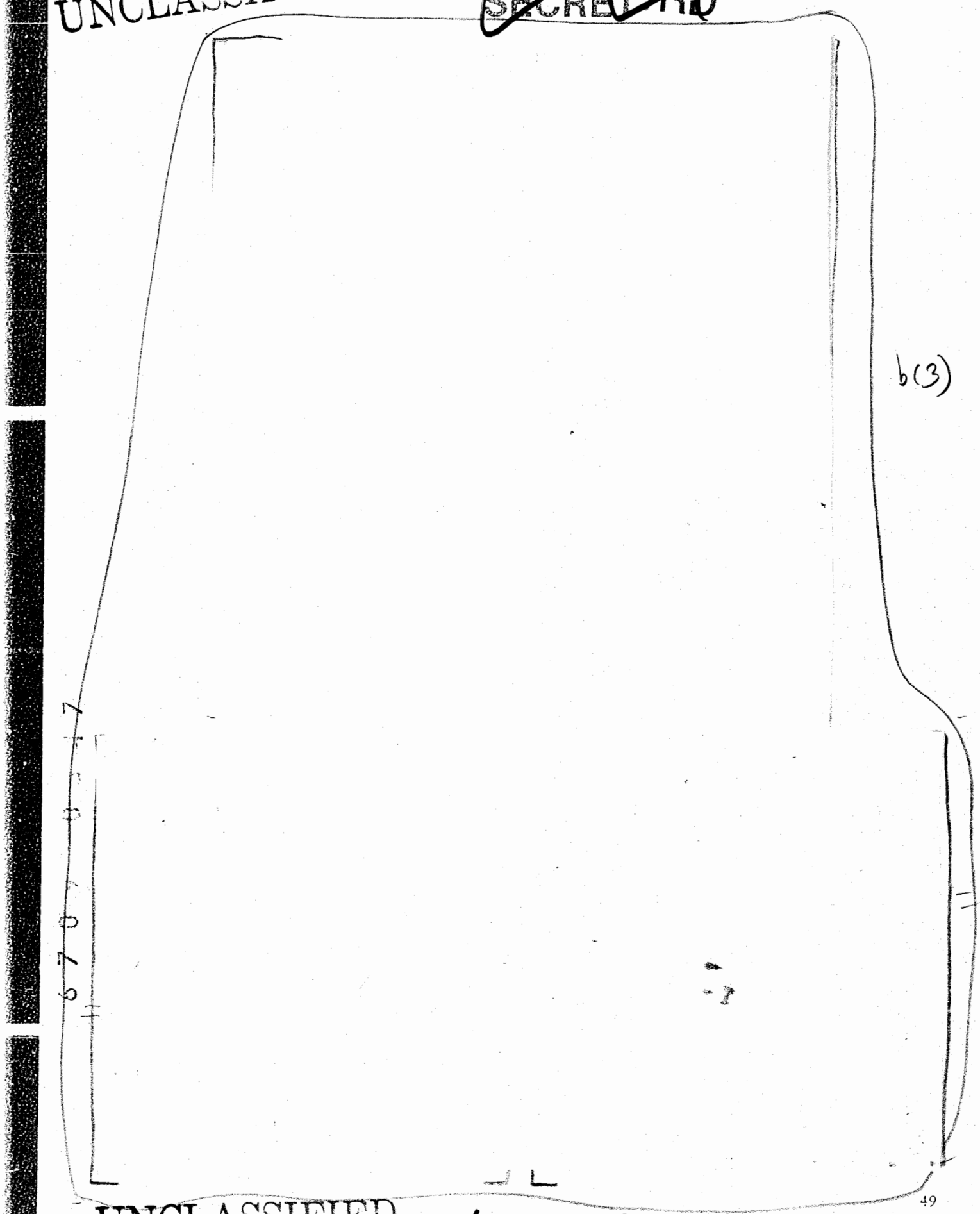

b(3)

UNCLASSIFIED SECRET AD

TABLE III. Diagnostic glossary

Nickname	Short Description

b(3)

b(3)

b(3)

Consequently, the height of the rack, which accordingly determines the location of the TV box, had to be increased to maintain the magnification.

Optimization of pinhole designs and rack height was achieved using existing codes to calculate performances of the stairstep taper pinhole design and the uniform taper design, both of which are shown schematically in Fig. 15. Final pinhole design parameters, shown in Table

UNCLASSIFIED SECRET AD

SECRET/RD

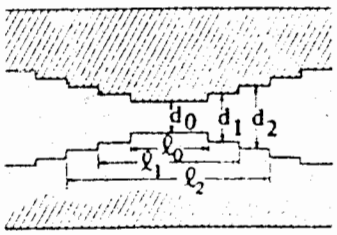

Conventional stair step

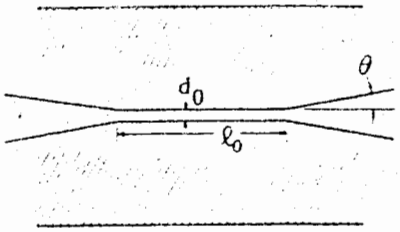

Uniform taper

b(3)

b(3)

b(3)

b

SECRET/RD

b13

b(3)

b(3)

UNCLASSIFIED
SECRET/BD

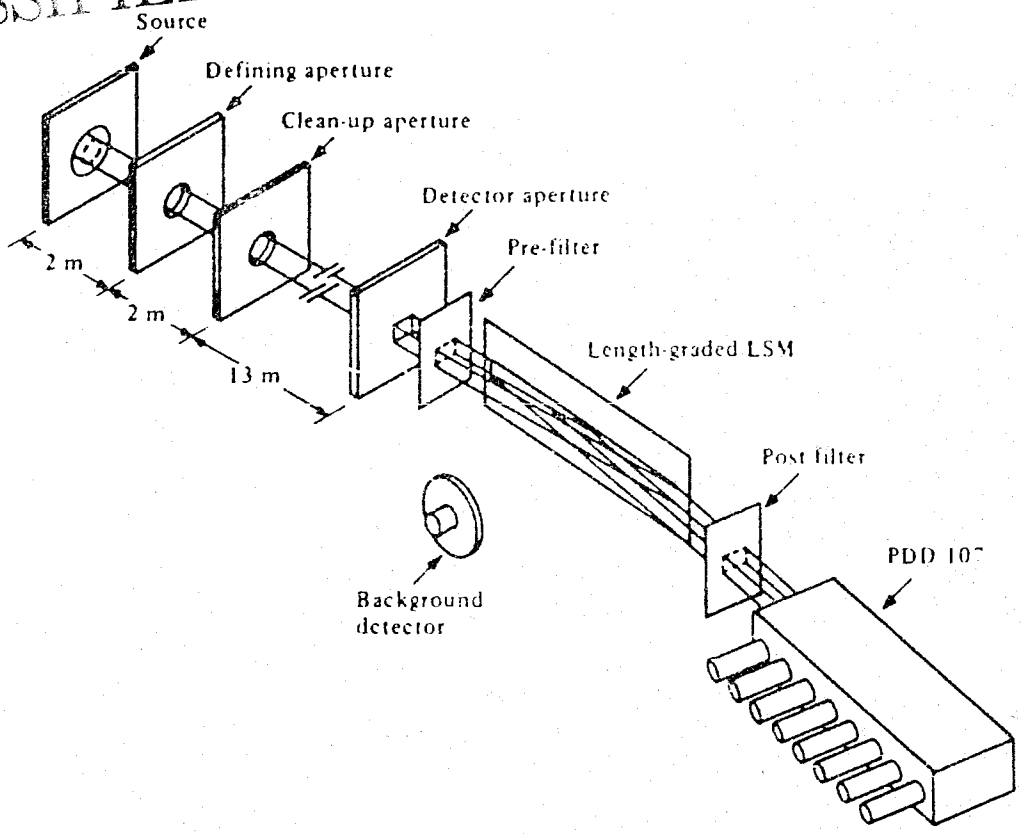

Fig. 17. SPEX LOS geometry.

The spectrometer was of novel design incorporating a synthetic x-ray diffraction crystal composed of alternating layers of carbon and palladium. The thickness of these layers was varied from one end of the crystal to the other so that 1.5-keV x rays were diffracted from one end while 2.5-keV x rays were diffracted from the other end of the flat crystal. The manufacture of these synthetic crystals was being worked on collaboratively by Los Alamos and Stanford University and represents a new class of x-ray optical elements that can be used in the design of x-ray diagnostics.

The detector used in this spectrometer was also of unique design and consisted of eight individual channels that intercepted different portions of the diffracted beam. The bandpass of each channel was determined by the fraction of the beam intercepted by each detector and the total energy spread across the beam. This design allowed us to build a moderate bandpass system with high throughput, relatively simple alignment, a very small single LOS, and a compact detector. Further extensions of this concept will allow us to perform routine measurements of x-ray spectra with moderate to high sensitivity and simpler and less expensive detector systems than are presently available.

[redacted] However, this restricted us to viewing only higher energy x rays.

b(3)

UNCLASSIFIED
SECRET/BD

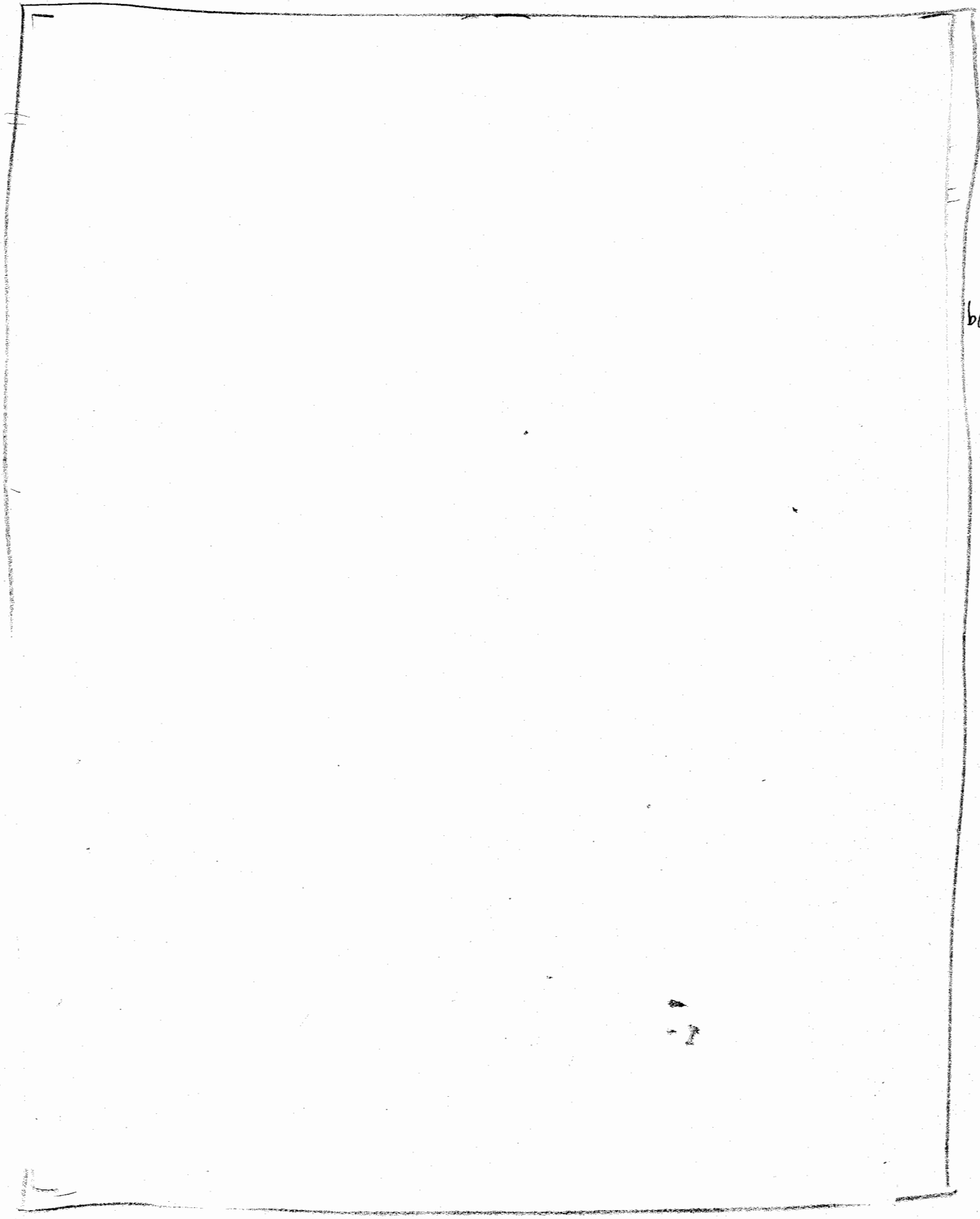

X-Ray Diagnostics

[redacted]

b(3)

The major differences in this experiment are engineering modifications aimed at reducing the cost of this experiment and simplyifying the vacuum system requirements.

[redacted]

b(3)

Ultrahigh vacuum conditions were maintained in the windowless detectors with appendage ion pumps on each x-ray detector. A thin vacuum window was placed in each detector forming the post filter for the channel. We avoided downhole high-voltage cables for each ion pump by implementing a distributed downhole, high-voltage power supply.

Further costs and complexity reductions were derived from deceasing the size of the LOS pipe to 6-in. diameter and utilizing K-F flanges on the roughing vacuum compatible sections. We also did not use an ultrahigh vacuum backup system.

[redacted]

b(

[redacted]

b(3)

b(3)

A synthesis of this resolution identified the camera, particularly the microchannel plate intensifier, as the largest contributor.

b(3)

FUTURE PLANS

The progress made to date in Centurion has created considerable enthusiasm and generated many objectives to pursue.

UNCLASSIFIED

SECRET/RD

APPENDIX A

COMPTION DETECTORS

Compton detectors were developed a little more than 20 years ago to meet a need in downhole diagnostic measurements for a detector with characteristics of ruggedness, very low sensitivity, high electrical bandwidth, and large dynamic range.

Two types of Compton detectors are in general use today: a thin vacuum variety with a thin center electrode developed by LLNL and a thick, oil-filled variety with a thick center electrode developed by Los Alamos.

The vacuum Compton diodes go by the generic designation VCD; there are various model numbers, mostly denoting the diameter of the central electrode (emitter). At present, there is only one type of oil-filled Compton detector in use, the HFK (High-Frequency Kenertium), so-called because of the 1-in.-thick Kenertium center electrode. (Kenertium is a machinable alloy of tungsten.)

Early versions of Compton detectors had only one output connector. However, it was discovered that putting two output connectors opposite each other more than doubled the electrical bandwidth at the expense of halving the sensitivity. This loss is no penalty when the observed source is a nuclear explosion.

Both types of detectors depend on the Compton effect for their operation, but the process is somewhat different in each case.

The conceptual design for a VCD is illustrated in Fig. 1A. Incident rays penetrate the thin entrance window (usually stainless steel) and cause Compton electrons to be emitted from the 4.8-mm-thick aluminum center electrode, resulting in a positive pulse propagation down the electrical cable. Neutrons have a similar effect; gamma rays are produced by (n,γ) reactions in the aluminum, again resulting in the emission of Compton electrons and a positive electrical pulse.

In the HFK, incident gamma rays produce Compton electrons in the oil; those within range of the Kenertium surface are collected by the electrode. The transmission through the electrode for gamma rays is ~10% so that the emission of Compton electrons from the back side o the electrode is down by a factor of 10 from the collec tion on the front side. Consequently, gamma rays resul in a negative electrical pulse. Neutrons produce knock on protons in the oil, to be collected by the electrode plus (n,γ) reactions in the Kenertium resulting in Compton electron emission. Both of these processes produce a positive electrical pulse. Hence, the HFK produces a negative electrical pulse for gamma rays and a positive pulse for neutrons, providing unambiguous signals. The reader should note that a theoretical treatment of the HFK should include ionization and polarization effects in the oil.

Compton detectors are operated with zero electrical bias. Because the detectors can have energies as high as several MeV, the detectors could, in principle, generate several-million-volt electrical pulses. In practice, the detectors become nonlinear at 5000 V across 50Ω (100 A) and saturate at about 20,000 V.

An early problem with VCDs was the emission of Compton electrons from the entrance window. This process causes a negative precursor to the detector step-function response and, in an extreme case of a particular gamma-ray spectrum, could result in zero output current. This problem was reduced to an acceptable level by using a thin entrance window, placing a lead electron stopper an appropriate distance in front of the detector, and putting an electron sweeping magnetic field between the lead and the entrance window.

The shaping of the ends of the electrodes shown in Fig. 1A gives an approximate match to the 50-Ω cable used to conduct the signals uphole.

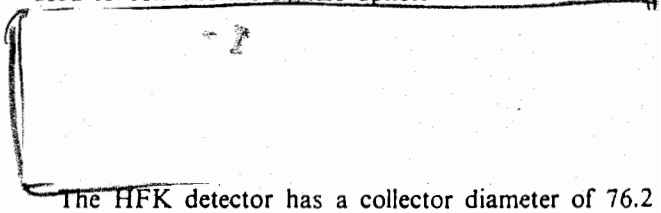

The HFK detector has a collector diameter of 76.2 mm and an electrical bandwidth of about 900 MHz.

UNCLASSIFIED

SECRET/RD

UNCLASSIFIED SECRET/RD

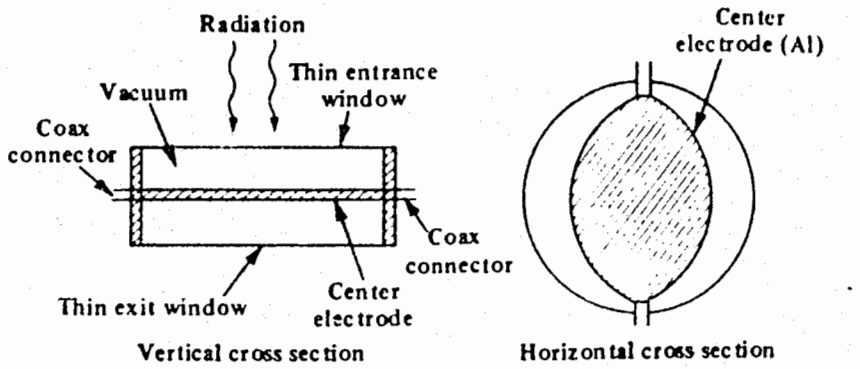

Vacuum Compton Diode (VCD)

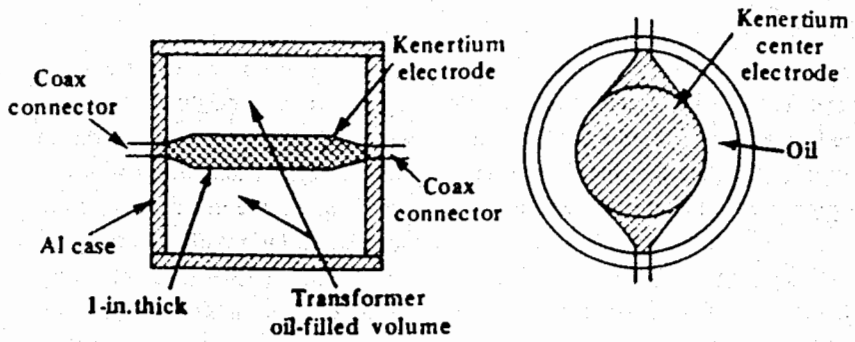

High-Frequency Kenertium (HFK)

Fig. 1A. Conceptual drawings (not to scale) of the design principles of the VCD and HFK detectors used for downhole diagnostics.

670 - 05869

UNCLASSIFIED SECRET/RD

SECRET/RD

UNCLASSIFIED

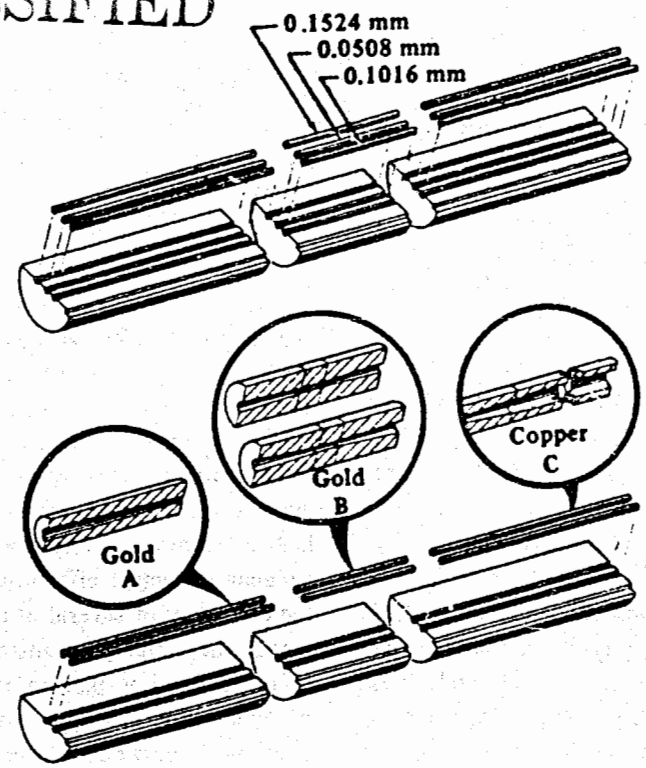

Fig. 1B. Manufacture of pinhole assemblies.

6709 0371

UNCLASSIFIED

SECRET/RD

SECRET/RD

UNCLASSIFIED

CO_2 LASER PLASMA INTERACTIONS

by David W. Forslund and Philip D. Goldstone

INTRODUCTION

The enormous pressures required to compress the inner portion of an Inertial Confinement Fusion (ICF) target to densities greater than the interior of the sun are accomplished by the conversion of the laser energy to x rays and particle energy in the plasma corona and by ablation of the target.

To achieve these compressions efficiently and effectively, we must understand the physics of matter from 10^{-5}-10^{3}g/cm^3 over distances of 10^{-5}-10^{0} cm and times of 10^{-5}-10^{-8}s with particle energies ranging from 0.1 to 10^{6} eV and magnetic fields ranging from none at all to 10^{3} T. The physics involved is nearly collisionless plasma physics including the effects of spontaneously generated magnetic fields, high-density collisional physics, the atomic physics of weakly to highly ionized materials, and their effects on transport of photons of all energies as well as particles. Frequently, the processes are far from equilibrium and require elaborate rate equations to describe their effects with reasonable accuracy.

Finally, we must understand thermonuclear burn, including the transport of all of the nuclear fragments, such as alpha particles, in the compressed fuel. We must be able to control radiation flow with a precision of a fraction of a per cent, and the hydrodynamic implosion may be complicated by the mixing of materials due to hydrodynamic instabilities and their subsequent effects on the thermonuclear burn process.

6 7 b(3)

In order to be a competitive, economical energy producer, the gain of the target must be as high as possible with the lowest possible energy input.

The biggest problem for inertial fusion in general, and laser fusion in particular, has been the mechanism of deposition of (laser light) energy into the target and subsequent transport of that energy to the ablation surface. The very properties of lasers that allow them to produce extremely high power and intensity (which is necessary for fusion) can work against a desirable form of energy deposition. In particular, the wave nature of the light, the high coherence, and narrow bandwidth all contribute to peculiar collective effects in the deposition that reduce the efficiency of several of the above processes. In other words, these highly organized properties of the laser tend to drive the hot plasma in the target far from thermodynamic equilibrium with potentially serious consequences. In particular, laser fusion with CO_2 lasers at 10 μm is dominated by such effects.

These collective mechanisms initially result in the production of energetic electrons by the absorption of laser radiation in the target corona. The hot-electron energy then cascades into a number of energy flow channels (magnetic fields, acceleration of energetic ions, bremsstrahlung emission, heating of a dense "thermal" plasma, soft x-ray emission, and microwave emission). Shorter wavelength laser-plasma interactions tend to be more collisional, and the collective processes which result in hot electrons, are generally less dominant.

Early in the history of laser fusion, researchers hoped to get quickly into the regime of significant thermonuclear burn. Many papers were published on the thermonuclear burn properties and the required conditions involving small amounts of fuel. Indeed, the energy required to compress and heat the fuel to ignition conditions is very small compared with the energy released. However, to achieve the necessary conditions of compression requires precise control of the input energy as the incident driver energy is decreased. Specifically, the very small fuel masses are susceptible to preheat, which will generate sufficient back pressure to prevent compression. Again, the smaller the fuel mass, the smaller the fraction of preheat allowed because one must compress to increasingly higher densities to accomplish fuel burn. The required precision of the implosion increase

SECRET/RD

UNCLASSIFIED

SECRET/RD

UNCLASSIFIED

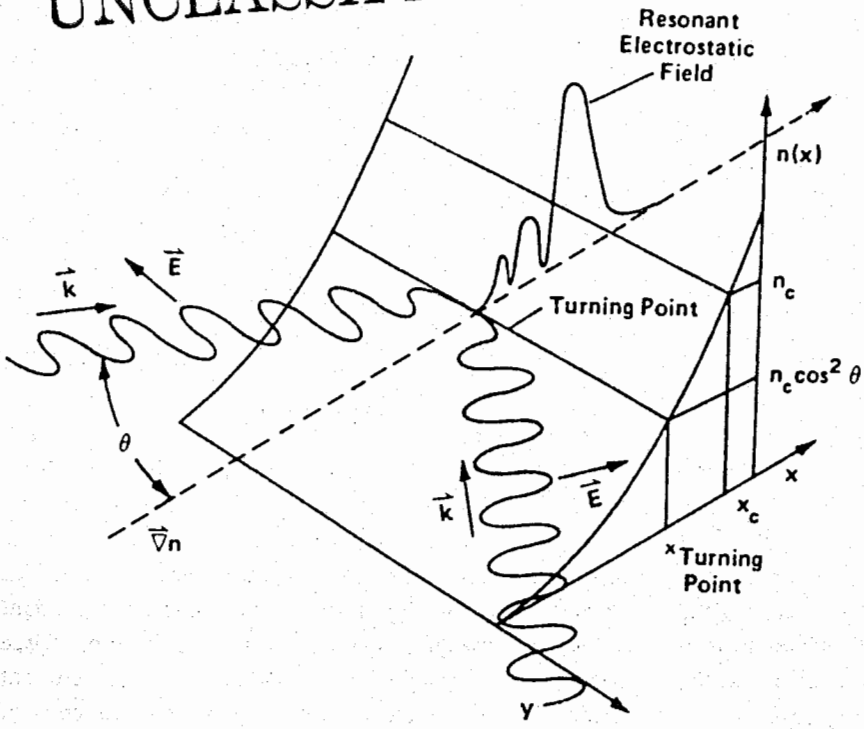

Fig. 2. The resonance absorption process.

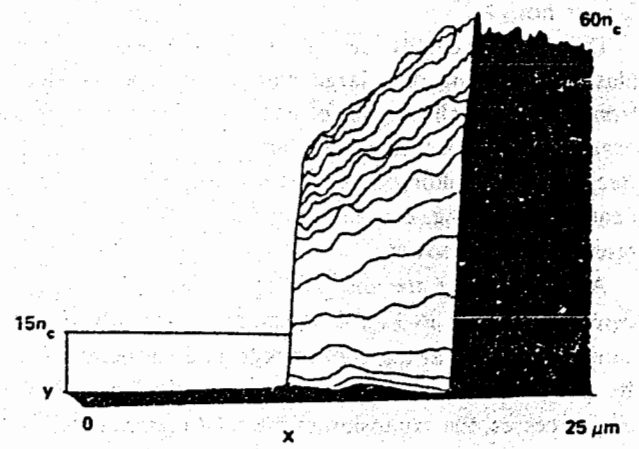

(a)

Fig. 3. Density gradients obtained from the WAVE code.

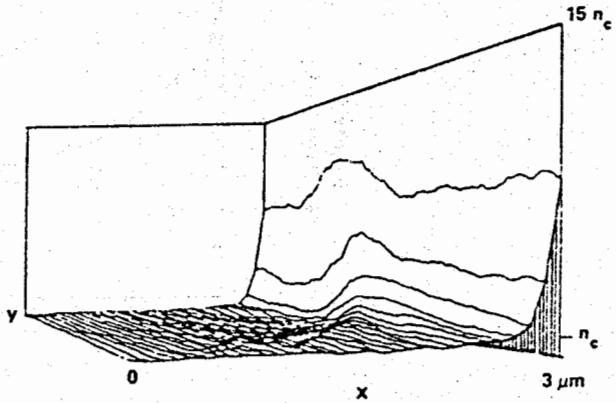

(b)

UNCLASSIFIED

SECRET/RD

UNCLASSIFIED

SECRET/RD

because of the greater mass of the ions, although it has the potential of reducing the absorbed laser intensity. Calculations suggest that the ion waves become nonlinear so rapidly that the light is not scattered away but merely adds to the plasma heating rate. This heating rate, however, is lower than that from electron plasma waves. This process may be much more important at short laser wavelengths, where the ion sound waves do not become as nonlinear.

In addition to backscattering, there are also self-focusing and filamentation instabilities of the incident light.[14] Pondermotive, force-driven filamentation has a similar gain length to Brillouin scattering when the ions are very warm, $T_i = T_e$. At low intensities there is a thermal, self-focusing instability resulting from bremsstrahlung heating that can reduce the density in a channel, refracting the light within the channel, which raises the intensity and further heats the plasma. This latter process may be particularly troublesome at short wavelengths. This instability can be viewed as arising from the strong anisotropy in the pressure of the incident light wave.

A number of parametric instabilities at the critical surface have been identified theoretically.[15] However, in general, the steep density gradients induced by the pondermotive force severely reduce these instabilities.

If fusion with CO_2 lasers is to work, one must stay at intensities and plasma conditions that do not allow parametric instabilities to develop and rely on resonant absorption in a steepened density gradient to maintain the lowest hot-electron temperature. These conditions appear difficult to achieve at best. As mentioned earlier, some additional absorption process appears to be occurring above 10^{15} W/cm^2. Recent simulations at an intensity of 2.5×10^{15} W/cm^2 run for tens of picoseconds instead of only a few picoseconds[4] (made possible by the substantial increase in size of the Los Alamos computer facility) show a similar phenomenon.

Figure 8 shows a contour plot of the density surface late in time. Note that the originally smooth, sharp density gradient has begun to break up and become rough. Associated with this roughness is a substantial increase in the absorption coefficient from about 25 to 60%. At the same time, the hot-electron temperature increases by a factor of 2 or 3 over that calculated for resonance absorption on the initially smooth surface. At 10^{16} W/cm^2, the surface is observed to become even more turbulent. Basically, the parametric instabilities at the critical density that were suppressed by the sharp gradient appear to become dominant at high intensity. This process may explain the increased hot-electron temperatures (hundreds of kiloelectron volts) observed on Helios at high intensities.[1,3]

We see then that the large amplitude of the laser radiation results in a highly nonequilibrium state of the plasma. It is so far from equilibrium that, for example, classical shock waves are altered. The region where resonant absorption occurs corresponds to a phase transition

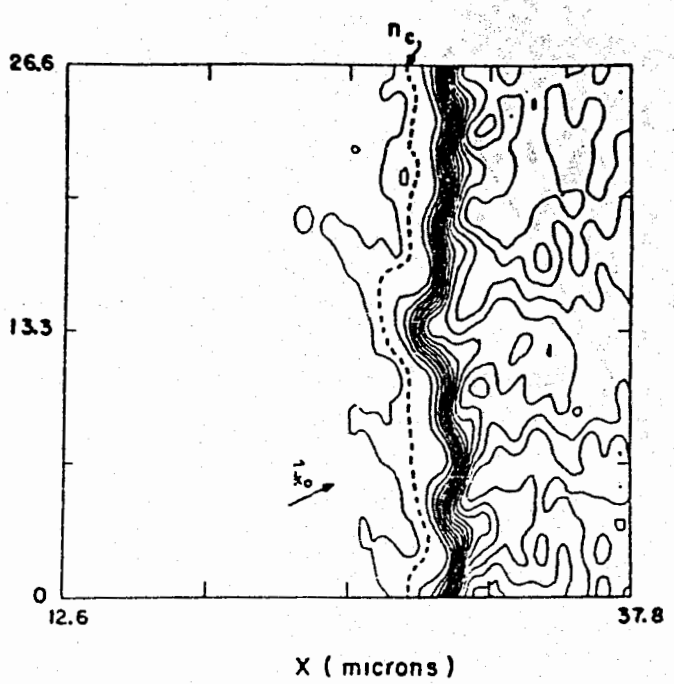

Fig. 8. Contour plot of the density late in time.

UNCLASSIFIED

SECRET/RD

SECRET/RD
UNCLASSIFIED

between a hot plasma in the presence of the laser light to a colder plasma without the laser light present. In this region, rarefaction shocks[16-18] are generated, which have very different properties from conventional shock waves. Matter is put into an extremely unusual state that is probably only reproduced in exotic astrophysical situations. The fact that most of the absorbed laser energy is placed into a few energetic particles significantly reduces the implosion efficiency of fusion targets and makes the task very difficult.

ENERGY FLOW

Hierarchy of Energy Flow Channels

Once hot electrons are produced by the absorption process, they proceed to convert their energy in one of two ways. Hot-electron pressure in the corona can collectively accelerate the coronal ions to extremely high energies by collisionless processes. In the simplest model, some electrons leave the target (they are initially ejected outward from the critical surface by the resonance-absorption mechanism), but the nonzero impedance and inductance of the target support stalk allow electrostatic potentials of hundreds of kilovolts to develop at the target, confining the remainder. The confined electrons accelerate ions by working against the coronal plasma as they try to escape.

Experimental measurement of the fast-ion energy shows that a substantial fraction of the absorbed laser light goes into fast ions, particularly at high intensity (Fig. 9). Alternatively, the electrons can lose their energy by collisional stopping in the bulk of the target. Because the range of hundred-kiloelectron-volt electrons in matter is quite long compared with the amount of material that can expand into vacuum under the influence of hot-electron heating during the laser pulse, the target material is to a first approximation isochorically heated. This collisionally deposited electron energy is partitioned into internal energy of the material, kinetic energy (thermal or "slow" hydrodynamic in contrast to the collisionless fast-ion expansion of the corona), and thermal, soft x-ray radiation.

If the target is thick compared with the hot-electron range, the motion of the target will be quasi-ablative. If the target is thin to electrons, it will explode. The collisional stopping of the hot electrons also produces hard x-ray bremsstrahlung[1,3] and characteristic x-ray emission,[19,20,21] which are not in themselves energetically important. However, they provide unique observables

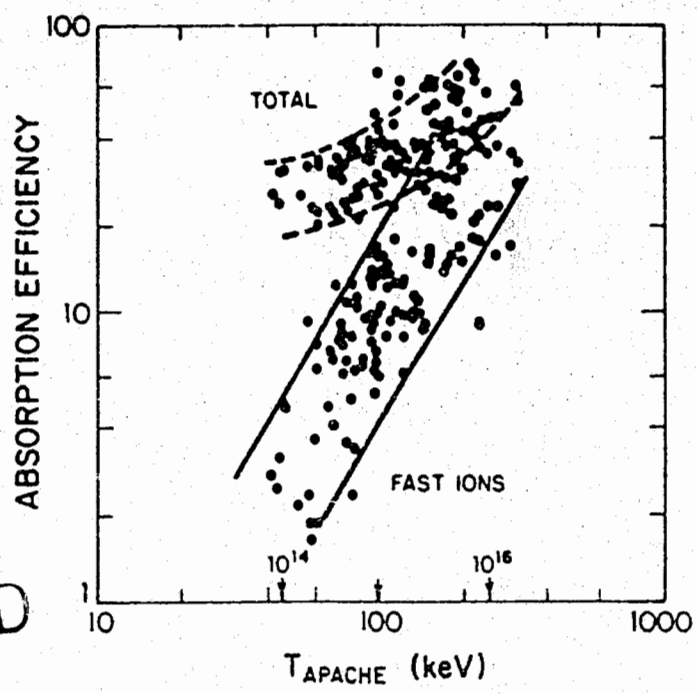

Fig. 9. Fast-ion production efficiency as a function of the hot-electron temperature (from the APACHE hard x-ray spectrometer) and intensity.

6 7 0 0 0 3 8 2
UNCLASSIFIED

SECRET/RD

that we have used to determine the hot-electron temperature, the amount of deposited electron energy, and the location where the hot electrons are depositing their energy.

Our experimental measurements, together with computer modeling, allow us to piece together a generally consistent picture of the energy budget and energy flow. The absorption, as noted above, can be as high as 60% at 10^{16} W/cm^2, although generally closer to 30% below 10^{15} W/cm^2. The energy partition to fast ions depends on a number of factors described below. However, because the energy partition to fast ions also increases with intensity (Fig. 9), the amount of energy that is collisionally deposited in, for example, a spherical target, is only about 20% of the incident radiation, independent of intensity. Ultimately, we wish to use one or more of these energy channels to provide energy to the ablator of a target capsule, either directly or indirectly, leading to the symmetric implosion of the capsule and thermonuclear burn. These basic energy channels also provide a "natural" set of observables we can use to trace the physical processes taking place: soft and hard x-ray emission; the fast-ion energy, spectrum, and angular distribution; and the slow- (thermal) ion distribution.

Fast Ions and the Energy Budget

Because fast ions can carry such a large part of the energy budget, we have studied these ions extensively with a wide variety of diagnostics. Many of the ion calorimeters that we have used to infer the absorption of laser light have been filtered with thin foils (typically 0.5-μm nickel) to detect only these fast ions and reject thermal ions and x rays. Such a filter will pass ions of 100 keV/amu (about 4×10^8 cm/s) with a weak dependence on the ion atomic number. In the simplest model of ion expansion, the ion distribution is an isothermal

$$N(v) = e^{-v/c_s} \cdot$$

with the sound speed driven by the hot-electron temperature

$$c_s = \sqrt{\frac{Z}{A} T_H} \cdot$$

For a hot electron temperature of 250 keV (obtained at 10^{16} W/cm^2) and for a Z/A = 1/2 appropriate for highly stripped ions such as carbon (for example, from a plastic target), the sound speed is approximately equal to the velocity of an ion that just passes through the filter. Because most of the ion kinetic energy is in ions above the sound speed, the ion energy transmitted through such a filter is a good estimate of the total fast-ion energy at high intensities, but at lower intensities where $c_s \ll 4 \times 10^8$ cm/s, this measurement is a lower bound.

The data in Fig. 9, in which the fraction of absorbed energy in the fast ions increases with intensity to as much as two-thirds of the absorbed energy, were obtained using filtered ion calorimeters as just described. The increase of fast ion fraction with intensity persists even after filter-thickness effects at lower intensities are estimated and corrections to the raw data in Fig. 9 are applied. Thus, the fast ions are a major energy channel and a major energy loss unless exploited for driving targets. The absorption (A) and the fraction of absorbed energy in fast ions (F) can be used to provide an indication of the energy remaining for collisional deposition, $E_c = A(1-F) \lesssim 0.25\ E_{inc}$, for spherical targets. Measurements of the ion velocity distributions with magnetic analyzer spectrometers [so-called Thomson parabolas, which are ion spectrometers with parallel E and B fields and which produce velocity spectra N(v) along parabolic tracks in the detector plane with different parabolas for each Z/A] indicate that much of the ion energy is carried by hydrocarbons independent of the target material. These hydrocarbons are surface contaminants on the target that are accelerated to the highest velocities because the lowest Z ions are accelerated most rapidly in the complex multispecies ion expansion. Although the ion spectrum from such a multispecies expansion is remarkably complex[22] and difficult to calculate theoretically, its gross properties are deceptively simple.

As the ion mean energy is not far above that required to penetrate a 0.5-μm nickel filter, we can determine the ion "spectrum" by a set of transmission measurements in an array of differently filtered calorimeters. Figure 10 shows examples of such ion spectra for high- and low-intensity cases. Not only are these transmission curves well behaved, they can readily be fit to an isothermal expansion model taking the hot-electron temperature T directly from the bremsstrahlung measurement if we assume $Z/A \approx 1/2$. Transmission data as in Fig. 1 are useful in evaluating target design concepts. For example, the mass required to stop one half of the ion energy is an important parameter that can be used to determine whether this ion energy is exploitable in target design.

Whereas ion stopping powers are a weak function of Z, very heavy ions (such as tantalum and gold) have an appreciably shorter range than protons or carbon. Based

can no longer free-stream into the target but are confined by the magnetic field. In VENUS simulations,[23] the electrons E × B drift along the target surface to great distances from the initial laser spot.[24] This reduces the transport inward under the laser spot and enhances the electron energy carried far from the laser spot. One of the consequences of the self-generated fields is that many of the ions are accelerated in an intense ion jet or plume normal to the target surface.

Figure 11 shows the angular distribution of ions leaving a disk target as measured by calorimeters with three different thresholds provided by filtering. The plume has half-width at half maximum of about 10°, in excellent agreement with particle simulations using VENUS. For targets smaller than about 1 mm, including small spheres, the effect is washed out and the ion angular distribution becomes more isotropic. The effect is also washed out in thin targets, where electrons can travel from the laser spot by reflexing through the shell and disrupting the current flow that creates the magnetic fields. For large, thick-walled spheres, however, the jets persist. Because in a spherical target experiment these jets will be directed back toward the focusing optics where they are not measurable, we believe that the apparent reduction in absorption in larger spheres as measured by calorimetry (Fig. 1) is due to this extremely forward-peaked, angular distribution. However, the appearance of a strongly directed ion jet, along with a large component of the energy budget in fast ions, raises the possibility that the ion energy might be directed from the laser target to the capsule and the ions used to drive the capsule either directly or indirectly.

TARGET DESIGNS TO EXPLOIT THE ENERGY FLOW

Because the details of the energy budget are in some measure affected by the target characteristics, we can design target concepts to use various energy channels and optimize them through design based on both empirical data and theoretical extrapolation.

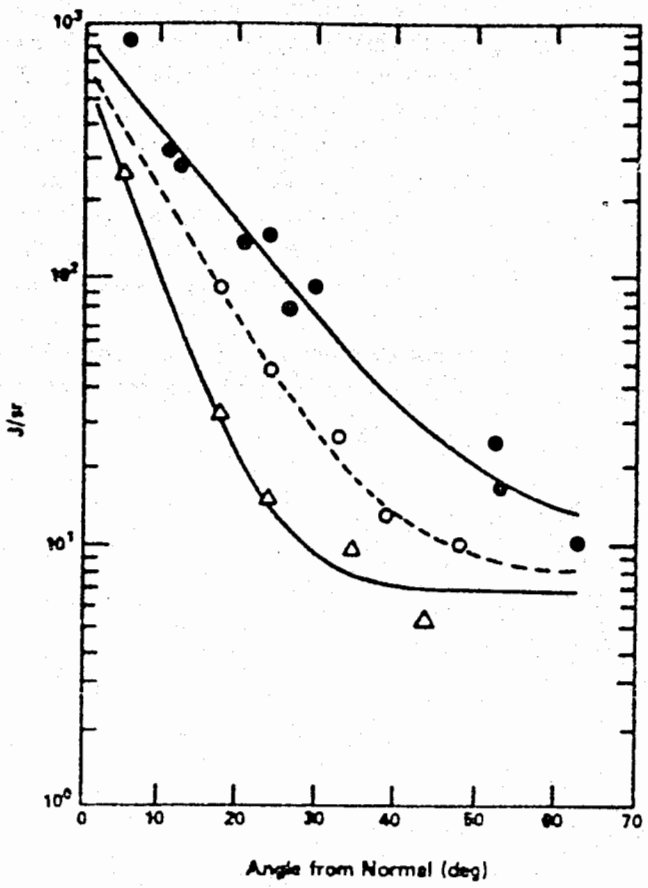

Fig. 11. Fast-ion angular distribution: • all ion energies, o E ≥ 100 keV/amu, Δ E ≥ 500 keV/amu.

SECRET/RD

UNCLASSIFIED

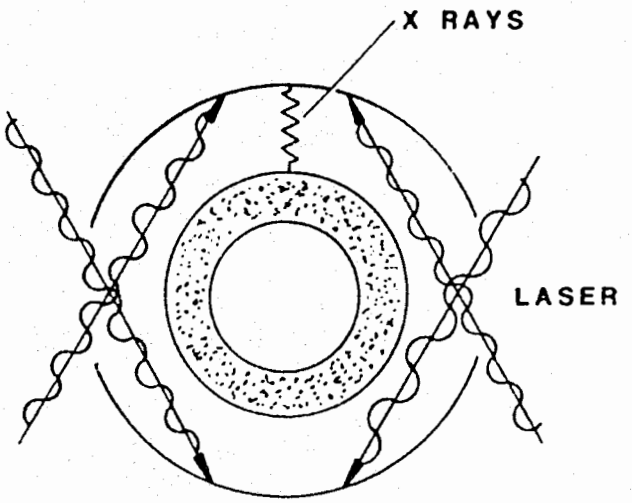

Fig. 13. Schematic of hohlraum target (Chamisa). Laser light is trapped inside case and absorbed, heating walls. Resulting x rays drive implosion. Issues are volume absorption of light by processes producing high, hot-electron temperatures, deep deposition of energy in walls, low efficiency of producing x-rays, and plasma closure of entrance holes.

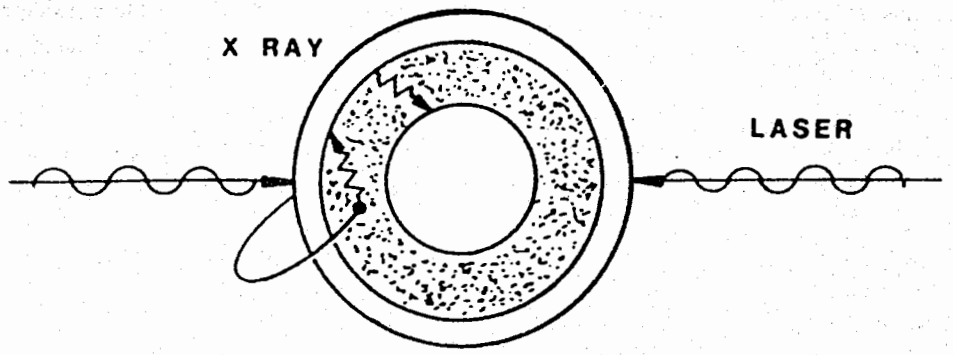

Fig. 14. Electron greenhouse target (Arcturus). Laser incident on high-Z case; hot electrons penetrate case and deposit in low-Z radiation generator/ablator. Radiation trapped inside case. Issues are low effective absorption, long range of hot electrons in ablator, resulting in low energy per unit mass, and coronal decoupling at long pulse suitable for high gain capsules.

5703 0588

Fig. 15. X-ray driven target using stagnation-produced x rays (Canopus). Hot electrons explode inner shell, which stagnates against wall of pod, converting kinetic energy to x rays, which enter main hohlraum containing capsule. Issues are high hot-electron temperature and loss of vacuum insulation, fast-ion production, and inefficient radiation flow from pod primary to secondary.

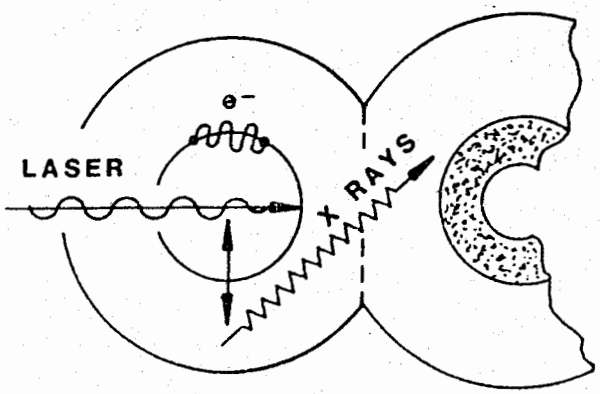

UNCLASSIFIED

SECRET/RD

UNCLASSIFIED SECRET/RD

Chamisa target, requiring the concept of "vacuum insulation." Hot electrons cannot move much beyond the leading edge of the ion expansion because of electrostatic effects (the same effects that, in fact, drive the ion expansion). Thus, if the space between the inner shell and outer pod wall is too small, the ions will cross the gap during the laser pulse; and the hot electrons, rather than exploding the inner shell, will be deposited in the pod wall. This situation will put a lower limit on the target size.

A major advantage that Canopus targets offer is that a short laser pulse (about 1 ns) can produce a long radiation pulse (about 10 ns) because of the change in characteristic times from that of the laser to that of the slow-ion stagnation. As target capsules generally desire long shaped pulses for optimum implosion efficiency and high compression, this concept provides an advantage by pulse shaping in the target rather than in the laser.

The Chamisa and Arcturus targets use the collisional deposition channel to produce x-ray drive. The direct-drive target uses this same channel to go directly to hydrodynamics (slow hydro). Canopus attempts to use both the collisional channel (to produce the slow hydro of the inner shell explosion) and the fast-ion channel. We can attempt to use both the high energy and beam-like nature of the fast ions to drive the final target type discussed here. In the Procyon target concept, the laser is incident at high intensity to maximize the fast-ion channel on an ion converter and acts as an ion diode, producing a beam of fast ions that can be directed toward an ion-driven target (Fig. 16). Because the fast-ion range is long, we utilize an ion-driven version of the greenhouse Arcturus target concept to turn the ion "beams" into x-ray drive.

There are a few other target concepts (we have studied nine in detail), but they are largely variants of these basic attempts to exploit the various energy flow channels available. Below, we summarize the ultimate performance of these targets based on an evaluation of Helios data. We then describe some of the experiments and the results we have used to reach our conclusions, thus briefly illustrating both the physics and the techniques used to unravel the problems.

ANALYSES OF TARGET DESIGN CONCEPTS

To evaluate the potential of these target design concepts, we chose to factor the problem into the capsule implosion physics and the drive mechanisms. In essence, we asked, "What is the efficiency with which one can provide the drive energy to the ablator?" We assumed that any drive concept could be made to produce the requisite drive symmetry. We also ignored—temporarily for this analysis—the effect of hot-electron or bremsstrahlung preheat on the capsule performance except as a constraint in target design (that is, in some cases we designed the target to limit the hot-electron penetration through the ablator, to the pusher, and to the fuel). We find that the resulting analysis does not crucially rest on these rather simple assumptions.

As most of our targets are x-ray coupled, we used a figure or merit called the x-factor to define the target coupling efficiency:

X = (x-ray energy absorbed by ablator)/(driver energy on target).

For direct drive, we converted to the effective x-factor by

$$X = (E_{abl}/E_{inc})(n_e/n_x) ,$$

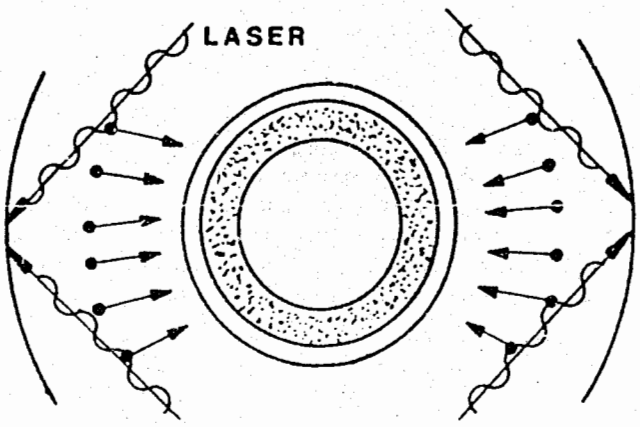

Fig. 16. Ion-beam coupled target (Procyon). High intensity CO_2 laser generates collimated jet of fast ions, which drive ion-driven, greenhouse target. Issues are efficiency of conversion to ion energy in the narrow jet.

5707 0387

UNCLASSIFIED

SECRET/RD

UNCLASSIFIED SECRET/RD

where $n_{e,x}$ are the "rocket" efficiencies for direct drive and x-ray drive for an equivalent amount of ablator energy. We estimated from systems studies and capsule gain calculations that $X > 0.25$ is necessary for fusion power production.

We note that for short-wavelength lasers (say, $\lambda = 0.25$ μm) in a Chamisa hohlraum target, the absorption is expected to be nearly 100% (absorption on open targets such as disks or spheres is almost that high) and as much as 80% of this energy may be converted to soft x rays.

About 10% of the x-ray energy is lost out the laser entrance holes; and of the remaining energy, about 60% is used to drive the heat front into the low-Z capsule ablator, and 40% is lost to the heat front in the high-Z radiation case. Therefore, for a short wavelength laser that is nearly ideal,

$$X \cong (1)\ (0.8)\ (0.9)\ (0.6) \cong 0.43\ .$$

Experiments at short wavelengths continue to be promising. Recent calculations indicate that the soft x-ray conversion expected may be somewhat less than the desired 80% when extrapolated to megajoule long-pulse experiments, indicating the need for continued experimentation and optimization.

In the Chamisa target, the absorption can be high and fast-ion loss can be small because energy must escape back out the laser entrance holes to be lost. At least 50% of the incident energy can be kept in the collisional channel. However, the hot-electron temperature in these hohlraums is extremely high (about 300 keV), much higher than expected for resonance absorption at the intensity of the laser beams as they first intercept the hohlraum wall. These hot electrons penetrate the hohlraum wall very deeply, and only a very small amount of the deposited energy resides within a radiation diffusion depth of the surface and is available for conversion to soft x rays. When the hohlraum is sized so that it does not fill with plasma above the CO_2 critical density during the long drive time required by the capsule (which would keep the light out of the target), scaling laws derived from Helios experiments indicate the low value of $X = 0.06$. Because the laser entrance ports must also be kept open and unfilled with plasma during the pulse, there is significant, additional loss of radiation out the holes. Thus, the x-factor for a Chamisa hohlraum, scaled to reactor size, is only about 0.02. In fact, more energy reaches the capsule in the form of preheating hot electrons than in the form of x rays.

In the Arcturus target, the basic limitation is the collisional deposition fraction, which for spheres is about 20 to 25% independent of intensity. Once we include the electron energy that does not penetrate the radiation case at the typical hot-electron temperature of 100 keV, only 18% of incident energy is deposited in the converter. To prevent hot-electron preheat of the pusher, much ablator mass is needed, lowering the temperature to which this mass can be raised to uninteresting value (tens of electron volts). Even using variations on the basic target design to work around the problem—the partition of the energy in the converter into internal energy and radiation and the efficiency of absorbing the radiation in the ablator rather than in heating the case—limits the x-factor for such a target to only $X \leqq 0.10$. Direct-drive targets are limited by the collisional-deposition fraction of 20 to 25% and the hydrodynamic efficiency of hot electron drive ablator relative to x-ray drive (a factor of 3 poorer), which gives $X = 0.08$.

In Canopus targets, all of the absorbed energy (which can be as high as about 80% in the inner hohlraum) can be converted to thermal and suprathermal hydro. However, the conversion to x-rays at the pod wall is inefficient, fast ions mostly go deeper in the pod wall than desirable, and extrapolation based on empirical scaling laws shows that only about 45% of incident energy reappears as thermal x rays. Of this relatively large fraction of the energy, about 22% is lost to heating the pod wall; 22% enters the main hohlraum where only about one-half, for an x-factor of 0.12, is finally deposited in the ablator. Whereas this is a higher x-factor than the concepts above, the scaling data that predict this eventual x-factor also predict that acceptable drive temperature in the main hohlraum requires significantly greater than 10 MJ in the laser pulse.

Procyon targets use the fast-ion channel, which at 10^{19} W/cm^2 takes <40% of incident energy. However, experiments have shown that only about 10% of incident energy is contained in the highly collimated ion jet, which can be transported to the capsule. The remainder of the ion energy is found at large angles in the wings of the peaked angular distribution. With the typical loss of efficiency in converting the ion energy to energy in the capsule ablator (similar to Arcturus), we have found the x-factor to be only 0.03 to 0.07.

This description summarizes the performance of the target concepts we investigated to exploit the various energy flow channels. Although there are a number of uncertainties in extrapolating our empirical data at <10 kJ

6 7 0 5 3 8

UNCLASSIFIED SECRET/RD

UNCLASSIFIED SECRET/RD

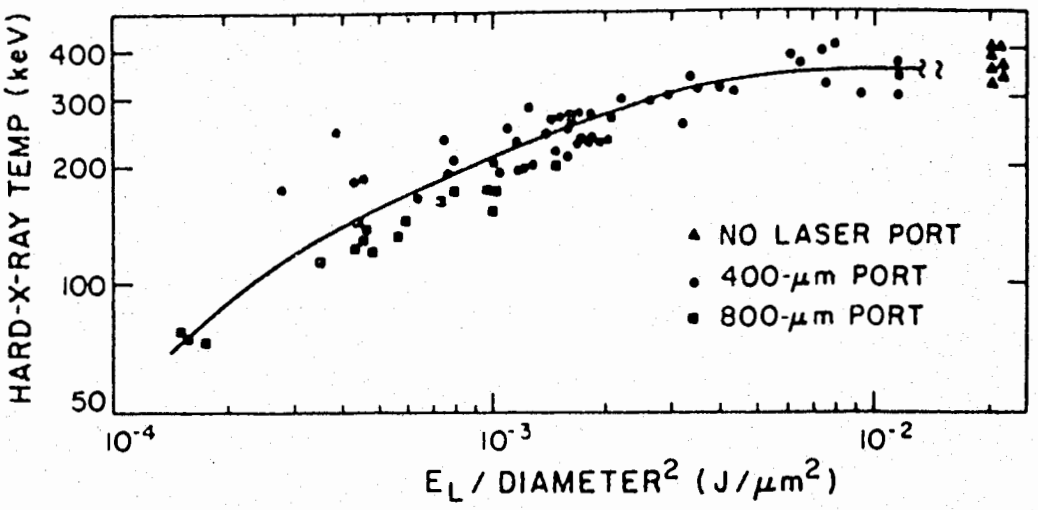

Fig. 20. Hot-electron temperatures for Chamisa hohlraums. Targets with 400-μm ports show saturation at high E/D^2, which may be due to hole closure.

Hot-Electron Range

To confirm this picture of the hot-electron transport in hohlraums, direct measurements of hot-electron transport in the hohlraum wall were made using hohlraums of copper and nickel layers (the copper on the inside, nickel on the outside). The copper was used as a variable-thickness electron attenuator. Characteristic inner-shell (K_α) x rays from the nickel are emitted at a rate roughly proportional to the energy deposition in the nickel. Thus, by observing the nickel K_α emission as a function of copper thickness, we can trace the specific deposition of electron energy as a function of depth in the wall. The targets were overcoated with 200 μm of CH to prevent false signals from being produced in the nickel by electrons migrating out of the hole to the target exterior.

The resulting electron range data (Fig. 21) can be well modeled using analytic electron transport calculations or LASNEX with a Maxwellian temperature close to the temperature measured by bremsstrahlung. In addition, quantitative fits of LASNEX calculations to the data are in general agreement with the measured energy balance for these experiments.

However, there is evidence for a small, additional component of electron energy with a lower temperature. This evidence comes from both K_α transport measurements and detailed x-ray spectra in the < 25-keV region on spheres and disks. From these measurements we infer a small enhancement of electron number at low-electron energies roughly sufficient to raise the near-surface energy deposition and, therefore, the wall radiation temperature from the LASNEX calculations to measured values.

Thus, the basic issues for CO_2-hohlraum scaling are hole closure and hot-electron temperature scaling. Our ability to understand the physics of these hohlraums is excellent with the exception of having few definitive measurements from which the mechanisms of hot-electron production can be determined. However, simulations indicate that Raman scattering is likely to be exceptionally virulent in the long-scale-length plasmas in these hohlraums. On one hand, very little scattered light indicative of Raman scatter is observed in our experiments. On the other hand, the simulations show that little scattered light is expected in these circumstances even when a large amount of laser light is absorbed through Raman processes.

Experiments with disk-and-washer hohlraum "mockups" showed increasing hot-electron temperature with increasing degrees of plasma confinement; that is, few hot electrons were produced with a washer (entrance port) alone, and few with a laser beam focused in front of a disk. However, when both disk and washer are present, providing some confinement of the disk plasma and allowing long scale lengths to develop, the hot-electron production rapidly increased. Experiments have also shown little change in the hot-electron temperature in

6709092
UNCLASSIFIED SECRET/RD

UNCLASSIFIED
SECRET RD

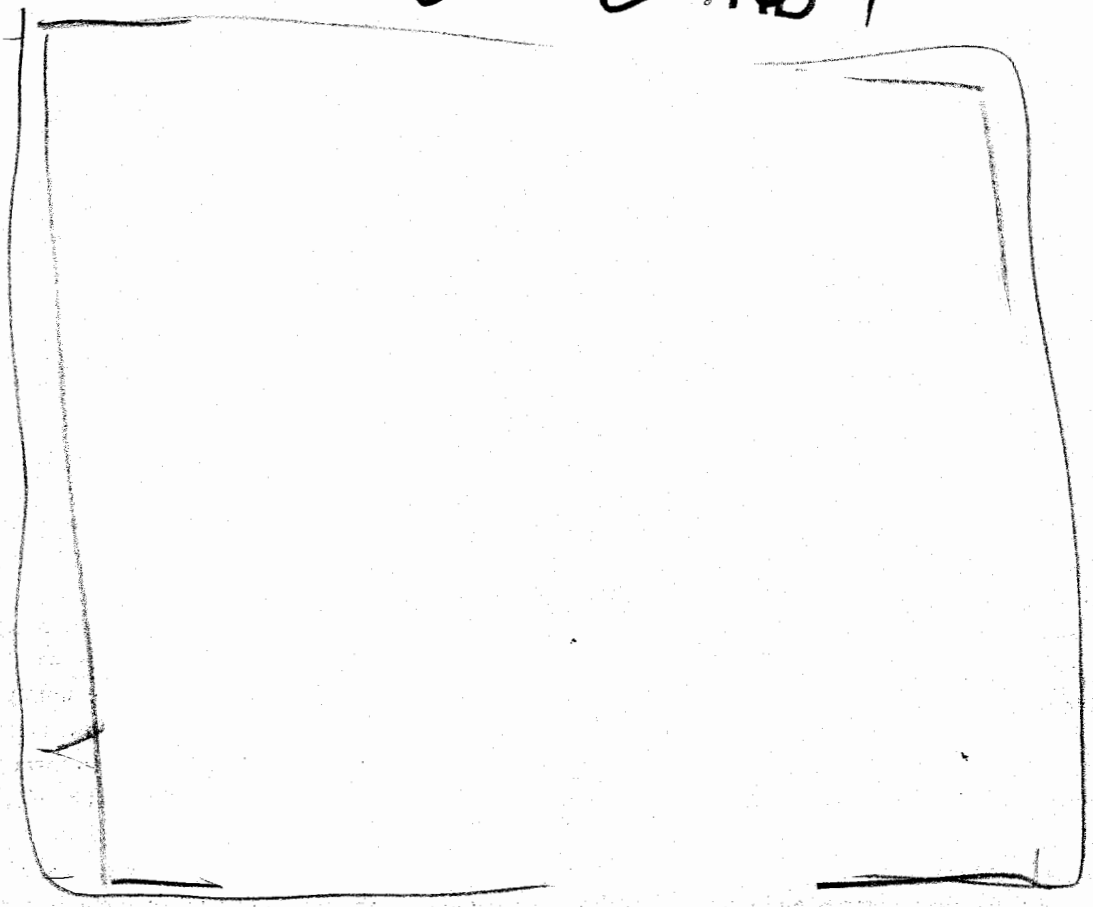

b(3)

Fig. 1. Schematic of a typical fusion target. As described in the text, each component plays a specific role in conversion of radiation from the driver to the implosive energy necessary for fusion of the fuel.

5705 0597

process produces tampers of very uniform thickness and great smoothness (Fig. 4). Electroless plating of substrates smaller than 500 microns in diameter is performed in an apparatus in which the spheres are kept in constant, random motion in a reaction chamber by alternating the flow direction of the metastable solution.[1,2]

Some recent target designs call for tampers of metals, such as beryllium and aluminum, that cannot be deposited from aqueous solution. We are therefore investigating deposition from organic solvents and possibly molten salts. The major obstacle in this research is the hazardous nature of such deposition media.

After the electroforming process, the substrate is removed from the tamper by leaching with an appropriate chemical through a hole drilled in the plating. The hole is then fitted with a separately fabricated plug containing small radial channels for entrance of the gaseous fuel. After the tamper is filled, the plug is sealed and joined to the tamper by laser welding, a process described in Ref. 3.

Antimix Layer

The antimix layer smooths the hydrodynamic instabilities generated in the outer shells of the target and thus helps achieve symmetric implosion. This layer consists of a full-density polymer, which may be cast and machined separately in the form of two mating hemishells or deposited directly on the tamper. Because we have discussed the former method in Ref. 3, we discuss here two methods for direct deposition of polymers from the gas phase: the low-pressure plasma (LPP) process and the vapor-phase pyrolysis (VPP) process. When fully developed, these processes will probably be the methods of choice for depositing antimix layers of the required thickness uniformity and surface smoothness.

In the LPP process a radio-frequency voltage between two electrodes produces a low-pressure plasma of the monomeric material, which then polymerizes on the tamper surface. Small tampers (less than 500 microns in

UNCLASSIFIED
SECRET RD

UNCLASSIFIED
SECRET/RD

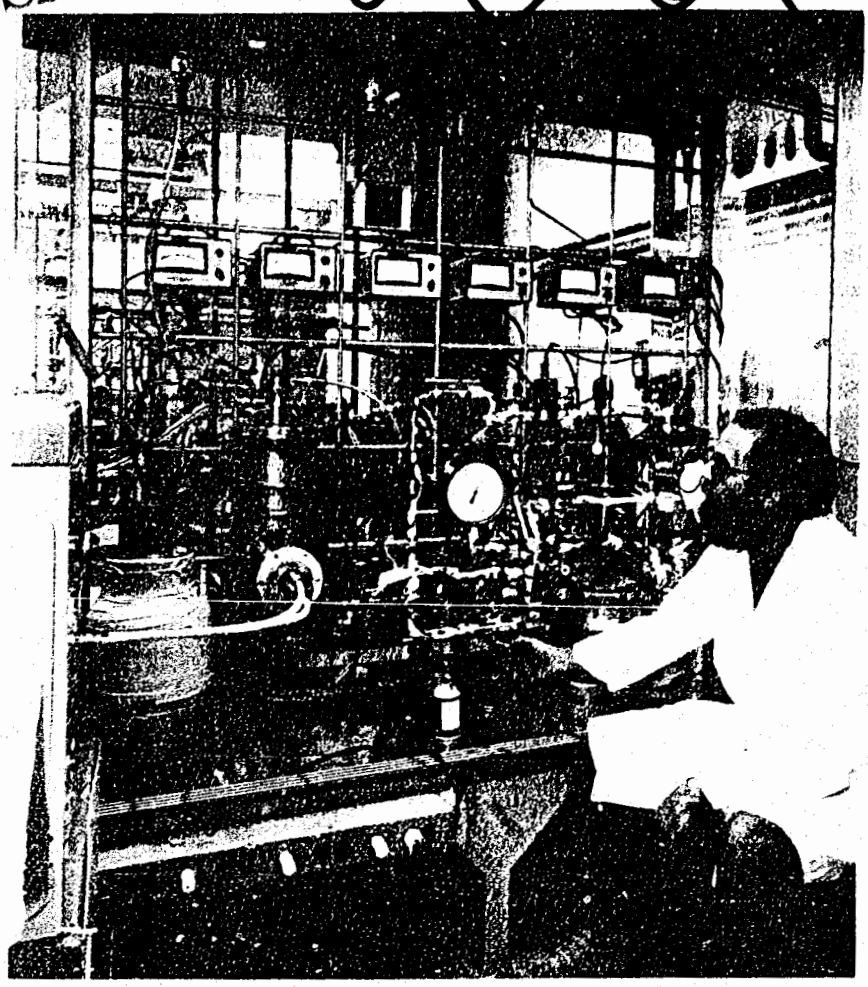

Fig. 12. Photograph of an apparatus for coating a fluidized bed of substrates by chemical vapor deposition. The fluidized bed is created in the cylindrical vessel heated by an external induction coil as the reactive gas flows upward through an orifice at the bottom of the vessel. The array of meters monitors process conditions such as gas flow and temperature.

REFERENCES

1. A. Mayer and W. Doty, "Advances in Plating and Forming Inertial Fusion Targets," in *Technical Digest-Conference on Inertial Fusion* (Opt. Soc. America, San Diego, California, 1980) p. 96.

2. A. Mayer and D. S. Catlett, "Plating Discrete Microparticles for Laser Fusion Targets," *Plating and Surface Finishing* (March 1978) p. 42.

3. H. Casey, W. R. Doty, R. Mah, A. T. Young, Jr., R. L. Rhorer, M. E. Kenyon, and G. A. Simonsic. "Capsule Fabrication (U)," in *Defense Science,* Los Alamos National Laboratory report LA-9140-PR (SRD) (May-August 1981) p. 53.

4. R. Liepins, M. Campbell, J. S. Clements, J. Hammond, and R. J. Fries, "Plastic Coating of Microsphere Substrates," *J. Vac. Sci. Technol.* 18(3), 1218 (1981).

5. A. T. Young, D. K. Moreno, and R. G. Marsters, "Preparation of Multishell ICF Target Plastic Foam Cushion Materials by Thermally Induced Phase Inversion Processes," *J. Vac. Sci. Technol.* 20(4), 1094 (1982).

6. R. L. Rhorer, "Update on Precision Machining at Los Alamos," in *Proceedings of the Society of Photo-Optical Instrumentation Engineers Annual Meeting*, San Diego, California, Vol. 433 (1983) p. 107.

UNCLASSIFIED
SECRET/RD